# LUND UNIVERSITY

**Alternative Lead Systems for Diagnostic Electrocardiography: Validation and Clinical Applicability**

Welinder, Annika

2009

[Link to publication]

Total number of authors:
1

# Alternative Lead Systems for Diagnostic Electrocardiography: Validation and Clinical Applicability

**AKADEMISK AVHANDLING**

som med vederbörligt tillstånd av Medicinska fakulteten vid
Lunds Universitet, för avläggande av doktorsexamen i
medicinsk vetenskap, kommer att offentligen försvaras i
Föreläsningssal 3, Centralblocket, Universitetssjukhuset i Lund,
torsdagen den 10 december 2009, kl. 09.00.

av

**Annika Welinder**

Fakultetsopponent:

Professor Peter Macfarlane
Universitetet i Glasgow, Storbritannien

LUNDS
UNIVERSITET
Medicinska fakulteten

| Organization LUND UNIVERSITY | Document name DOCTORAL DISSERTATION |
|---|---|
| | Date of issue 2009-12-10 |
| | Sponsoring organization Region of Scania; Kristianstad; the Faculty of Medicine, Lund University, Lund; and Philips Medical Systems, Oxnard, California. |
| Author(s) Annika Welinder | |

| Title and subtitle |
|---|
| Alternative Lead Systems for Diagnostic Electrocardiography: Validation and Clinical Applicability |

**Abstract**

The standard 12-lead electrocardiogram (ECG) is one of the most important and most frequently used tools for diagnosing cardiac diseases. The standard ECG uses 10 electrodes placed on well-defined positions on the body, 6 placed on the torso and 4 placed distally on the limbs. The waveform patterns and the criteria for interpretation are taught in medical school.

In several situations, such as during exercise or long-term monitoring, use of the electrode positions of the standard ECG is not optimal because of the abundance of artifacts. In these situations, the limb electrodes must be placed proximally, often even on the torso, and the Mason–Likar (M–L) positions are commonly used. Interference with other clinical procedures can also constitute a problem. Therefore, an ECG-recording system with fewer electrodes and without any electrodes on the limbs that provides a 12-lead ECG similar to the standard ECG would be valuable, and the so-called EASI system is such an alternative lead system.

Physicians who use ECGs in their day-to-day work are often not aware of the differences between 12-lead ECGs recorded from standard versus alternative electrode positions, and they might use criteria developed for the standard ECG when interpreting an ECG obtained from an alternative lead system. This can lead to misinterpretation with the risk of potentially serious consequences for the patient. Because limb electrodes cannot always be placed distally, optimizing the proximal positions for better concordance with the standard ECG would be of great value for improved diagnostic performance. A version of the "Lund" (LU) lead system has been reported to agree better with the standard lead system than does the M-L lead system. To develop a uniform convention for ECG recording, a recording must produce waveforms that have morphologies approximating those obtained with standard ECG and that have noise immunity close to that of M-L.

The overall objectives of this thesis were 1) to further validate the EASI system to gain more knowledge about the agreement between EASI-derived and standard 12-lead ECGs, and 2) to investigate the possibility of optimizing the positions of proximally placed limb electrodes.

The thesis increases the knowledge about the agreement between EASI-derived and standard 12-lead ECGs, and indicates that the EASI-derived ECG might be a possible alternative to standard ECG also in children. The results further indicate that the LU system might constitute a uniform convention for resting as well as monitoring ECG applications.

| Key words: ECG, alternative lead systems, monitoring, diagnosis, uniform convention |
|---|

| Classification system and/or index termes (if any): |
|---|

| Supplementary bibliographical information: | Language |
|---|---|

| ISSN and key title: 1652-8220 Alternative Lead Systems for Diagnostic ECG | ISBN 978-91-86443-04-7 |
|---|---|

| Recipient's notes | Number of pages 144 | Price |
|---|---|---|
| | Security classification | |

# Alternative Lead Systems for Diagnostic Electrocardiography: Validation and Clinical Applicability

## ANNIKA WELINDER, MD

**LUND UNIVERSITY**
**Faculty of Medicine**

Doctoral Thesis
2009
Department of Clinical Physiology
Lund University, Sweden

**Faculty opponent**

Professor Peter Macfarlane, University of Glasgow, UK.

The public defense of this thesis will, with due permission from the Faculty of Medicine at Lund University, take place in lecture room 3, Lund University Hospital, on Thursday, 10 December 2009, at 9:00 a.m.

Cover:

*Heart - Zackarias Welinder*

annika.welinder@med.lu.se

Department of Clinical Physiology, Lund University,
221 00 Lund, Sweden

Carpe Diem!

# Contents

# List of Publications

This thesis is based on the following publications, which are referenced in the text by their Roman numerals.

I.   Pahlm O, Pettersson J, **Thulin A**, Feldman CL, Feild DQ, Wagner GS. Comparison of waveforms in conventional 12-lead ECGs and those derived from EASI leads in children. *J Electrocardiol* 2003:36:25–31.

II.  **Welinder A**, Feild DQ, Liebman J, Maynard C, Wagner GS, Wettrell G, Pahlm O. Diagnostic conclusions from the EASI-derived 12-lead electrocardiogram in children. *Am Heart J* 2006;151:1059–1064.

III. **Welinder A**, Sörnmo L, Feild DQ, Feldman CL, Pettersson J, Wagner GS, Pahlm O. Comparison of signal quality between EASI and Mason-Likar 12-lead electrocardiograms during physical activity. *Am J Crit Care* 2004;13:228–234.

IV.  **Welinder AE**, Wagner GS, Horáček BM, Martin TN, Maynard C, Pahlm O. EASI-derived vs standard 12-lead ECG for Selvester QRS score estimations of chronic myocardial infarct size, using cardiac magnetic resonance imaging as gold standard. *J Electrocardiol* 2009;42:145–151.

V.   **Welinder A**, Wagner GS, Maynard C, Pahlm O. Diagnostic accuracy and immunity to noise of 12-lead ECG waveforms acquired from monitoring electrode positions. *Manuscript*.

# Summary

The standard 12-lead electrocardiogram (ECG) remains one of the most important and most frequently used tools for diagnosing cardiac diseases, although several different examination modalities in cardiology have been developed over the years. The standard ECG uses 10 electrodes placed on well-defined positions on the body, 6 on the torso and 4 distally on the limbs. Both industry and academia have invested many years in development of the criteria used to interpret the "diagnostic" standard ECG, and the waveform patterns are taught in medical school.

In several situations, however – such as during long-term ECG monitoring or stress testing – use of the electrode positions of the standard ECG is not optimal because of the abundance of noise. In these situations, the limb electrodes must be placed proximally, often even on the torso, and the Mason-Likar (M-L) positions are commonly used. Interference with other clinical procedures, such as echocardiography, can also constitute a problem. An ECG-recording system with fewer electrodes and without any electrodes on the limbs that provides a 12-lead ECG similar to the standard ECG would be valuable. The so-called EASI system uses only 4 recording electrodes in easily determined locations on the torso from which the full 12-lead ECG can be derived. The 12-lead ECG derived from the EASI system has been evaluated in adults in several clinical situations.

Physicians who use ECGs in their day-to-day work are often not aware of the differences between 12-lead ECGs recorded from standard versus alternative electrode positions, and they might use criteria developed for the standard ECG when interpreting an ECG obtained from an alternative lead system. This can lead to misinterpretation with the risk of potentially serious consequences for the patient. Optimizing the proximal positions for better concordance with the

standard ECG would be of great value for improved diagnostic performance. A version of the "Lund" (LU) lead system has been reported to agree better with the standard lead system than does the M-L lead system, with regard to both Q-wave width and QRS frontal plane axis. To develop a uniform convention for ECG recording, i.e. both for diagnostic ECG and for monitoring, a recording must produce waveforms that have morphologies approximating those obtained with standard ECG and that has noise immunity close to that of M-L.

The overall objectives of this thesis were 1) to further validate the EASI system to gain more knowledge about the agreement between EASI-derived and standard 12-lead ECGs, and 2) to investigate the possibility of optimizing the positions of proximally placed limb electrodes.

*EASI studies*

In *Study I*, age-specific transformation coefficients were determined for use in deriving 12-lead ECGs from the EASI signals. The agreement of the waveforms between simultaneously recorded standard and EASI-derived 12-lead ECGs in children (healthy and with various cardiac diagnoses) was studied. For children, it was better to use age-specific transformation coefficients than adult coefficients. The agreement between standard and EASI-derived ECGs was mostly good.

In *Study II*, the intrareader variation of interpretations of 2 standard 12-lead ECGs was compared with the variation of interpretations of standard versus EASI-derived 12-lead ECGs in children (*Study I* population). The variation of the interpretation of standard versus EASI-derived ECGs was only slightly larger than the intrareader variation of interpretations of standard ECGs.

In *Study III*, the amplitudes of myoelectric noise and baseline wander were compared between simultaneously recorded EASI-derived and M-L 12-lead ECGs in healthy adults. Overall, the 2 lead systems had similar susceptibilities to baseline wander, but EASI was less susceptible than M-L to myoelectric noise.

In *Study IV*, differences in the estimated size of myocardial infarction (MI), as assessed by Selvester scores, were compared between standard and EASI-derived 12-lead ECGs among patients who had had an episode of chest pain suggestive of an acute coronary syndrome. These scores were also compared with MI size measured by cardiac magnetic resonance imaging (MRI). Estimated MI size did not differ significantly between the 2 lead systems, but neither the correlation nor the agreement between MRI and either of the 2 lead systems was very strong.

*Study to optimize the proximal positions of the limb electrodes*

In *Study V*, waveforms from the LU and M-L systems were compared with those from standard ECGs with regard to the QRS axis in the frontal plane and QRS changes of inferior MI. The noise immunities of the standard, LU, and M-L systems were also compared. LU produced ECG waveforms that more closely resembled those obtained with standard ECG than did M-L. The LU system was more noise-immune than was the standard system, and the noise immunities of the LU and the M-L systems were comparable.

# Populärvetenskaplig sammanfattning

Standard-12-avlednings-EKG är fortfarande ett av de viktigaste och vanligaste redskapen för att diagnostisera hjärtsjukdom trots att ett flertal olika undersökningstekniker har utvecklats under åren. Vid standard-EKG används 10 elektroder, 6 på bröstkorgen och 4 distalt på armar och ben. Inom både industrin och akademin har många års arbete lagts ned på utveckling av de tolkningskriterier som används vid tolkning av ett "vilo"-standard-EKG och det är EKG-mönstren vid standard-EKG som lärs ut under läkarutbildningen

I flera situationer är det dock inte optimalt att använda standard-EKG pga riklig förekomst av muskelstörningar, t ex vid registrering av EKG under en längre tid eller vid arbetsprov. I dessa situationer placeras arm- och benelektroderna vanligen proximalt, ofta på bröstet, och s.k. Mason-Likar (M-L) placering är vanligt förekommande. Standardelektrodplaceringen kan också interferera med och därmed utgöra problem vid andra undersökningar, såsom ultraljudsundersökning av hjärtat. Ett alternativt EKG-system med färre elektroder och utan elektroder på armar och ben, som resulterar i ett 12-avlednings-EKG snarlikt standard-EKG vore värdefullt. Vid det s.k. EASI-systemet används endast 4 registreringselektroder på lätt identifierbara punkter på bröstkorgen, från vilka samtliga 12 avledningar kan beräknas. EASI-systemet har utvärderats för vuxna i flera kliniska situationer och befunnits vara väl användbart.

Ett problem är att läkare som dagligen använder EKG i sitt kliniska arbete ofta inte är medvetna om de skillnader som finns mellan 12-avlednings-EKG registrerade från standard respektive alternativa elektrodpositioner och använder de kriterier som utvecklats för standard-EKG även när de tolkar EKG från alternativa avledningssystem. Detta kan leda till feltolkningar och få konsekvenser för de berörda patien-

terna. Eftersom distal placering av arm- och benelektroderna inte alltid är möjlig, skulle optimering av de proximala positionerna, för bättre överensstämmelse med standard-12-avlednings-EKG, vara av stort värde för förbättrad diagnostik. En version av det s.k. Lund (LU)-avledningssystemet har rapporterats stämma bättre överens med standard-EKG än vad M-L gör, avseende både den s.k. Q-vågsbredden och den s.k. elektriska axeln. För att nå en enhetlig konvention för EKG-registrering, i vila och under längre tid, måste en registrering ha ett EKG-utseende som är mycket likt det som erhålls från standard-EKG och störningskänslighet åtminstone motsvarande den hos M-L.

Avhandlingens övergripande mål var 1) att ytterligare utvärdera EASI-systemet och därmed vinna mer kunskap om överensstämmelsen mellan EASI-beräknat och standard-12-avlednings-EKG, samt 2) försöka optimera placeringen av proximalt placerade arm- och benelektroder.

*EASI-studier*

I *studie I* utvecklades åldersspecifika konstanta faktorer som används för att beräkna 12-avlednings-EKG från EASI-signalerna. Överensstämmelsen hos vågformationerna mellan samtidigt registrerade standard- och EASI-beräknade 12-avlednings-EKG hos barn (friska och med olika hjärtfel) studerades. För barn visade det sig bättre att använda åldersspecifika konstanta faktorer än de faktorer som används för vuxna. Överensstämmelsen mellan standard- och EASI-beräknade EKG var mestadels bra.

I *studie II* jämfördes variationen i tolkningen av ett standard-12-avlednings-EKG från en gång till en annan med variationen i tolkningen mellan standard- och EASI-beräknade 12-avlednings-EKG hos barn (samma studiepopulation som i *studie I*). Variationen i tolkningen mellan standard- och EASI-EKG var endast något större än gång till gång variationen i tolkningen av standard-EKG.

I *studie III* jämfördes utslagen från muskelstörningar och s.k. baslinjevariationer mellan samtidigt registrerade EASI-beräknade och M-L-12-avlednings-EKG, hos friska vuxna. Totalt sett hade de två avledningssystemen likartad känslighet för baslinjevariationer, men

16

jämfört med M-L-systemet var EASI-systemet mindre känsligt för muskelstörningar.

I *studie IV* jämfördes skillnaderna i s.k. Selvesterpoäng (ett mått för att utifrån EKG beräkna hjärtinfarktstorlek) för genomgången hjärtinfarkt från standard- och EASI-beräknade 12-avlednings-EKG hos patienter som haft en episod med bröstsmärta talande för akut hjärtsjukdom. Dessa poäng jämfördes med uppmätt hjärtinfarktstorlek vid magnetkameraundersökning (MRI). Det var ingen signifikant skillnad i Selvesterpoäng mellan standard och EASI, men varken sambandet eller överensstämmelsen mellan MRI och respektive EKG-avledningssystem var särskilt stark.

*Studie för att optimera proximala placeringen av arm- och benelek-troder*

I *studie V* jämfördes EKG-vågor från LU- och M-L-systemen med dem från standard-EKG, med avseende på den elektriska axeln i fron-talplanet och EKG-förändringar som tyder på inferior hjärtinfarkt. Störningskänsligheten hos standard-, LU- och M-L-systemen jämför-des också. LU-systemet gav EKG-utseende som bättre stämde överens med standard-EKG, än vad EKG-utseendet från M-L-systemet gjorde. Vidare var LU-systemet mindre störningskänsligt än standard-systemet och störningskänsligheterna hos LU- och M-L-systemen var jämförbara.

# Abbreviations

BSPM        body surface potential mapping
DE-MRI      delayed enhancement magnetic resonance imaging
ECG         electrocardiogram, electrocardiography
IHD         ischemic heart disease
LU          Lund lead placement system
MI          myocardial infarction
M-L         Mason-Likar lead placement system
MRI         magnetic resonance imaging
RMS         root-mean-square
VCG         vectorcardiogram, vectorcardiography
WCT         Wilson central terminal

# 1 Introduction

## 1.1 Electrocardiography: a historic retrospective

The first electrocardiogram (ECG) in a human was recorded by Waller[1] in 1887. He strapped a pair of electrodes on the front and back of the torso, or inserted the right hand and right foot into jars of salt solution, and connected an electrometer (an instrument that measured electrical potential). The mercury in the electrometer moved at each beat of the heart. Until Einthoven[2,3] introduced the 3 limb leads – I, II, and III – in the early 20th century, however, the ECG was not used for diagnostic purposes. In the beginning, the patient's distal arms and legs were inserted into jars of conducting solution to provide optimum interface between the body and the insensitive recording device. It was then possible to measure the difference in electrical potential between the 2 arms, between the right arm and left leg, and between the left arm and leg.

Today, the convention remains to place the limb electrodes distally on the arms and legs for a "diagnostic" ECG recording. Lead I registers the potential difference between the left and right arms, lead II registers the potential difference between the right arm and left leg, and lead III registers the potential difference between the left arm and leg. The sum of the potentials in leads I and III equals the potential in lead II at any instant in time; this relationship is known as Einthoven's law. Einthoven developed the clinical analysis of the ECG during the early 20th century, and he was awarded the Nobel Prize in Physiology or Medicine in 1924 for his contributions to the development of electrocardiography.

In the early 1930s, Wilson et al. introduced the concept of a "central terminal."[4] The Wilson central terminal (WCT) is the average of the potentials at the left arm, the right arm, and the left leg.

A virtual reference point was thus created, making it possible to measure the potential difference between any point on the body and this reference (Figure 1.1). Because the WCT has a relatively constant potential throughout the cardiac cycle, the resultant waveform varies mainly according to the potential at the given electrode.[5]

In 1938, the committees of the American Heart Association and the Cardiac Society of Great Britain and Ireland jointly recommended the routine use of a single precordial lead placed upon the extreme outer border of the apex beat, determined by palpation.[6] The same year the Committee of the American Heart Association for Standardization of Precordial Leads described 6 precordial electrode positions as we know them today (Figure 1.2).[7] The precordial leads record the cardiac activity in a (slightly tilted) transverse plane from the right ventricle to the lateral wall of the left ventricle.
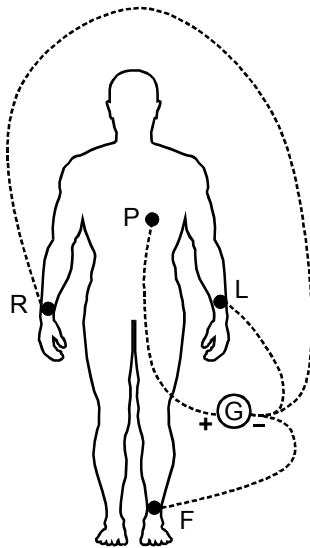
FIGURE 1.1 A precordial lead is derived using the WCT. L = left, R= right, F = foot, P = precordial electrode, and G = galvanometer.
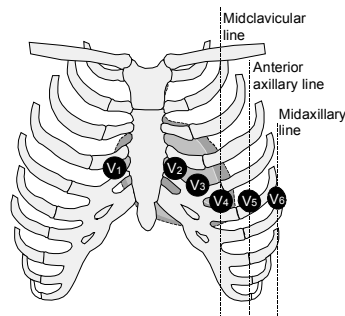
FIGURE 1.2 Electrode positions for the precordial leads, V1–V6.

The limb leads, labeled VR, VL, and VF, were generally of low voltage. In 1942, Goldberger introduced a modification of the WCT to amplify these voltages.[8] The modified WCT consists of the average of the potentials at the 2 limbs not being explored; thus, if the potential difference between the left arm and the modified WCT is measured, the reference point consists of the average of the potentials at the right arm and left leg. This modification of the WCT increased the potential of the unipolar limb leads by 50%, so they were denoted as "augmented limb leads" and labeled aVR, aVL, and aVF. The relationship between the augmented limb leads as well as between the nonaugmented limb leads is that the sum of the potentials recorded by the 3 leads is 0 at any given time.

The potentials of the limb leads represent directions in the frontal plane, from –30° to +120°, separated by intervals of 30° (Figure 1.3). These directions are based on the Einthoven triangle[3] which is in itself, however, an approximation. In Sweden, –aVR (the inverted aVR lead) is preferred to aVR, and the lead sequence aVL, I, –aVR, II, aVF, and III is most often used. This is a more logical sequence for displaying the leads than the conventional one (I, II, III, aVR, aVL, and aVF). The logical sequence is known as the Cabrera (panoramic) presentation.[9]
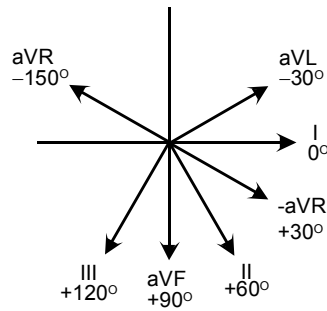
FIGURE 1.3 Directions of the limb leads in the frontal plane. 0° is arbitrarily defined to be in the direction of lead I.

Computer-aided ECG recording has become standard during the last few decades. In the 1960s, computerized acquisition and interpretation of the ECG were introduced, and are today incorporated in almost all modern ECG-recording devices.

The 3 limb leads (I, II, and III), the augmented limb leads (aVR, aVL, and aVF), and the precordial leads (V1–V6) together form the standard 12-lead ECG, which still is the most widely used system for ECG recording. The standard 12-lead ECG, with its electrode placement distally on the limbs, forms the basis for both manual and automated electrocardiographic analysis and remains one of the most important and most frequently used tools for diagnosing cardiac diseases. For several clinically important diagnoses, e.g. acute coronary syndrome, the standard 12-lead ECG is of crucial importance to confirm or rule out the diagnosis and to guide treatment decisions. The ECG, with at least 2 recording electrodes, is the most important tool for determining the cardiac rhythm. Figure 1.4 illustrates the positions of all the electrodes of the standard 12-lead ECG.

Figure 1.5 illustrates the normal appearance of a tracing from lead V5 of the standard 12-lead ECG. The P wave represents the depolarization of the atria, and the QRS complexes represent the depolariza-

tion of the ventricles. The distance between the P wave and the QRS complex represents the conduction time between the atria and the ventricles. The T wave represents the repolarization of the ventricles. The repolarization of the atria occurs during the depolarization of the ventricles, and the wave representing this is usually hidden within the QRS complex.
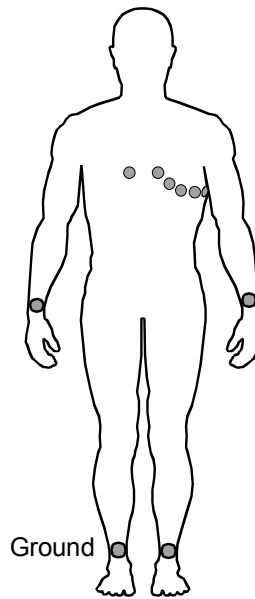


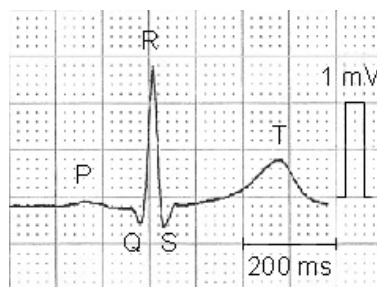FIGURE 1.4 Electrode positions for the standard 12-lead ECG.



FIGURE 1.5 The normal appearance of lead V5.

## 1.2 Alternative lead systems

### *The Frank system*

A vector is an entity that has a specific magnitude and direction. The basic idea of the vectorcardiogram (VCG) is that, for every instant, the electrical activity in the 3-dimensional heart can be summarized to 1 vector. The size and direction of the vector change as a function of time during the cardiac cycle. By convention, the left-to-right component of the vector is called X, the caudal-cranial component of the vector is called Y, and the posterior–anterior component of the vector is called Z. If the amplitudes (x, y, and z) for each component (X, Y, and Z) are known at any instant of time, pairs of these (xy, xz, and yz) can be plotted on the respective axes, and thus a vectorcardiograpic "loop" in each orthogonal plane (the frontal, XY, the transverse, XZ, and the sagittal, YZ, planes) can be obtained. The depiction of these 3 loops makes up the VCG. The shape, area, and direction of rotation of the loops are then analyzed.

In 1956 Frank presented a lead system for VCG recording, which was the first truly corrected orthogonal lead system;[10] that is, the lead vectors associated with the system were indeed orthogonal. The Frank system measures the potential variations from 7 well-defined positions: 5 on the torso (A, C, E, I, and M), 1 on the back of the neck (H), and 1 on the left foot (F) (Figure 1.6). Leads A, C, E, and I are placed in the same transverse plane, in the fourth or fifth intercostal place. A and I are placed in the left and right midaxillary lines, respectively; E and M are placed on the sternum and spine, respectively; and C is placed between E and A. The nomenclature of the electrode positions was derived from the concept of labeling points around the chest at intervals of 22.5°, starting from the center of the body and position A, and moving anteriorly.

Frank constructed a torso model with the dimensions of a medium-sized man (weight, 79 kg; height, 1.79 m), filled it with salt water, and placed a dipole in the position of the heart. With the dipole directed to the left, downwards, or backwards, he measured voltages for about

200 positions on the surface of the torso. The results from these experiments[11] underlie the equations from which the 3 orthogonal leads (X, Y, and Z) are generated. Today, few medical practitioners are familiar with the technique of VCG.
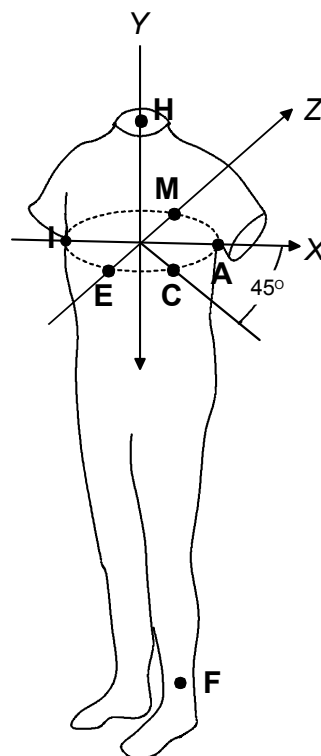


FIGURE 1.6 Electrode positions of the Frank system.

## The EASI lead system

When the acquisition and interpretation of the ECG became computerized, the storage requirements and time required for data transfer and analysis were all markedly reduced if only 3 leads were used instead of 12. However, most clinicians wanted to see a 12-lead ECG. Dower

et al. introduced a method for deriving a 12-lead ECG from the VCG.[12] Mathematically, each of the leads is expressed as a linear combination of the orthogonal X, Y, and Z leads:

$$\text{Derived lead} = aX + bY + cZ,$$

where a, b, and c represent fixed coefficients. The X, Y, and Z potentials represent simultaneous measurements from each of the leads at one particular instant; thus this calculation must be carried out at each sampling instant.

The Frank system, with electrodes on the back of the torso and on the back of the neck, is not practical for monitoring. The EASI lead system of Dower et al.,[13] is probably the most frequently used derived 12-lead system at present. This system requires only 4 recording electrodes, and their positions are shown in Figure 1.7. Positions A, E, and I are those of the Frank VCG system. Lead E is placed on the lower end of the sternum, leads A and I are placed on the left and right mid-axillary lines, respectively, in the same transverse plane as E, and lead S is placed on the sternal manubrium. The term EASI was constructed from rearrangement of the electrode labels.



FIGURE 1.7 Electrode positions of the EASI lead system.

Three quasi-orthogonal ECG leads are yielded by pairwise subtraction of the signals recorded at the E, A, S, and I sites:

$$AI = V_A - V_I$$
$$ES = V_E - V_S$$
$$AS = V_A - V_S$$

Lead AI views the electrical activity of the heart in a left-to-right direction (X). Lead ES views the electrical activity of the heart in a caudal-cranial direction (Y), and also contains a c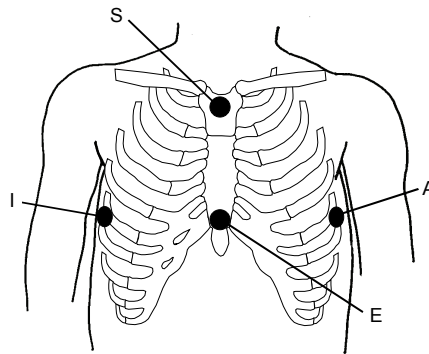onsiderable posterior–anterior component (Z). Lead AS views the electrical activity of the heart in both left-to-right and caudal-cranial directions (X and Y) and contains a small posterior-anterior component (Z). The 12-lead ECG is then derived by linear combination of the quasi-orthogonal ECG leads as described above. Dower did not publish explicit transfer coefficients, however; this was done later by Feild et al.[14]

Similar to modified 12-lead ECGs from other alternative lead systems,[15–17] the EASI-derived 12-lead ECG has the disadvantage of altering the resulting ECG waveforms compared with the standard 12-lead ECG. The transition zone (where the QRS complexes change from being predominantly negative to being predominantly positive) in the EASI-derived 12-lead ECG often occurs between leads V2 and V3, whereas in the standard 12-lead ECG, it generally occurs between lead V3 and V4. The QRS voltages also tend to be slightly smaller in the EASI-derived 12-lead ECG, especially in the precordial leads, compared with those of the standard 12-lead ECG.[18] However, the EASI-derived 12-lead ECG achieves high agreement with the standard 12-lead ECG (standard or proximal limb lead placement) in detection of myocardial ischemia[19–23] and other cardiac abnormalities[19] and in classification of arrhythmias.[18,19] A prior study has indicated the utility of the EASI-derived 12-lead ECG compared to just the 3 EASI leads, AI, ES, and AS, with regard to information on arrythmias in Holter recordings.[24] Few studies have examined the EASI lead system in children.

### *The Mason-Likar lead system*

Excessive noise, mainly due to the distal placement of the limb electrodes, has made it impractical to use the standard 12-lead ECG with distal limb leads for ECG monitoring. The limb electrodes are now usually placed on the torso to attain acceptable noise levels, and the Mason-Likar (M-L) modification of the standard 12-lead ECG[25] is commonly used for ECG monitoring. The M-L lead system uses all the conventional precordial electrode sites, but the limb electrodes are positioned on the anterior part of the torso instead of on the distal limbs (Figure 1.8).



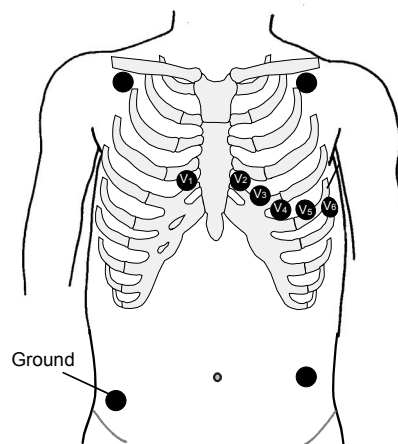FIGURE 1.8 Electrode positions of the M-L lead system. The right and left arm electrodes are positioned in the right and left infraclavicular fossae, respectively, medial to the border of the deltoid muscle and 2 cm below the lower border of the clavicle. The left leg electrode is positioned in the anterior axillary line, halfway between the costal margin and the crest of the ilium. The ground electrode can be placed anywhere.

Fundamental differences between the M-L 12-lead ECG and the standard 12-lead ECG include rightward shift of the QRS axis in the frontal plane; reduction of R-wave amplitude in leads I and aVL; increase of R-wave amplitude in leads II, III, and aVF; and poor reproduction of variables indicating especially chronic inferior myocardial infarction (MI).[15,17] The R-wave amplitudes in the precordial leads are also altered as a result of moving the 3 limb electrodes onto the torso. These differences can have clinical significance in the interpretation and serial comparison of diagnostic ECGs recorded with different limb electrode placements. Unfortunately, the misconception persists among physicians that the M-L and standard lead systems produce essentially identical waveforms.

### *The Lund lead system*

The Department of Clinical Physiology at Lund University Hospital has used the Lund (LU) lead system for exercise tests with bicycle ergometry for many years.[15] This lead system uses all the conventional precordial electrode sites, but the limb electrodes are positioned on the lateral side of the left and right arm at the level of the axillary folds, and on the left iliac crest in the anterior axillary line. The differences between the LU and the standard lead systems were found to be much less pronounced than were the differences between the M-L and standard lead systems.[15] This is in good agreement with the findings of Wilson,[26] in that the magnitude of potential differences decreases with increasing distance from the heart only until the attachment of the limbs to the torso; there is no further appreciable drop in potential along the limbs. Moving the left leg electrode of the LU lead system to the major trochanter of the left femur (Figure 1.9) diminishes the potential differences between this system and the standard 12-lead system.[16]

Many physicians are unaware of the nonequivalence of ECG recordings made with standard limb electrode positions versus proximal limb electrode positions, and therefore use the interpretation criteria developed for the standard positions when interpreting all ECGs. This can lead to misinterpretation with risk of consequences for the patient.

Given that the distal limb placement of the electrodes cannot be used in all situations, optimizing the positions of proximal limb electrodes for better concordance with the standard 12-lead ECG would have great value in improving diagnostic performance, and in achieving the objective of having a uniform convention for diagnostic ECG recording and for ECG monitoring. To develop such a convention, a recording must produce waveform morphologies that are close to those obtained with the standard ECG and that has noise immunity close to that of the M-L system. Large noise levels lead to false-alarm situations that are very disturbing for the nursing staff and that can compromise patient safety.
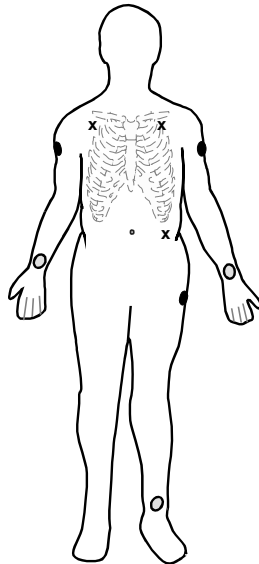


FIGURE 1.9 Electrode positions of the limb leads of the LU (●), the M-L (X), and the standard lead systems (○).

### *Body surface mapping*

The 10 electrodes of the standard 12-lead ECG cover only a small part of the body surface. Body surface potential mapping (BSPM), a technique that uses a larger number of electrodes to cover more of the body surface, was introduced to permit better resolution of the spread of excitation and recovery through the heart. Waller published the first study within this area in 1889.[27] Present-day systems vary greatly in the number and placement of recording sites.

Compared with the standard 12-lead ECG, BSPM has higher sensitivity for the diagnosis of chronic MI and left ventricular hypertrophy, and can better localize accessory atrioventricular pathways in patients with Wolff-Parkinson-White syndrome.[28–30] However, Carley et al. showed that the use of BSPM resulted in only a small increase in sensitivity and a corresponding decrease in specificity for the diagnosis of acute MI compared with the standard 12-lead ECG.[31]

BSPM is primarily used for research, and no standards have been established for the lead systems. It is seldom used clinically because of the time required to record the large number of signals, and because of the difficulty to assess the large quantity of information.

## 1.3 The Selvester QRS scoring system

The Selvester QRS scoring system estimates MI size in the left ventricle by a quantitative evaluation of QRS changes in the standard 12-lead ECG.[32] Based on computer simulation of the electrical activation sequence of the human heart, Selvester et al. originally developed a 57-criteria, 32-point QRS scoring system.[33] Wagner et al. then evaluated intra- and interobserver variability in humans for a simplified version of the system containing 37 criteria and 29 points.[34] The system was evaluated and modified through a series of studies[35–39] into the present 50-criteria, 31-point system[40–42] based on QRS changes in 10 of the 12 leads (Figure 1.10); each point corresponds to infarction of approximately 3% of the left ventricular myocardium. To investigate

| Lead | Criteria | Pts. |
|---|---|---|
| I [2] | Q ≥ 30 ms | 1 |
| | R/Q ≤ 1 | 1 |
| | R ≤ 0.2 mV | 1 |
| II [2] | Q ≥ 40 ms | 2 |
| | Q ≥ 30 ms | 1 |
| aVL [2] | Q ≥ 30 ms | 1 |
| | R/Q ≤ 1 | 1 |
| aVF [5] | Q ≥ 50 ms | 3 |
| | Q ≥ 40 ms | 2 |
| | Q ≥ 30 ms | 1 |
| | R/Q ≤ 1 | 2 |
| | R/Q ≤ 2 | 1 |
| V1(ant) [1] | Any Q | 1 |
| (post) [4] | R/S ≥ 1 | 1 |
| | R ≥ 50 ms | 2 |
| | R ≥ 1.0 mV | 2 |
| | R ≥ 40 ms | 1 |
| | R ≥ 0.6 mV | 1 |
| | Q and S ≤ 0.3 mV | 1 |
| V2(ant) [1] | Any Q | 1 |
| | R < RV1 | 1 |
| | R ≤ 10 ms | 1 |
| | R ≤ 0.1 mV | 1 |
| (post) [4] | R/S ≥ 1.5 | 1 |
| | R ≥ 60 ms | 2 |
| | R ≥ 2.0 mV | 2 |
| | R ≥ 50 ms | 1 |
| | R ≥ 1.5 mV | 1 |
| | Q and S ≤ 0.4 mV | 1 |
| V3 [1] | Any Q | 1 |
| | R ≤ 20 ms | 1 |
| | R ≤ 0.2 mV | 1 |
| V4 [3] | Q ≥ 20 ms | 1 |
| | R/Q ≤ 0.5 | 2 |
| | R/S ≤ 0.5 | 2 |
| | R/Q ≤ 1 | 1 |
| | R/S ≤ 1 | 1 |
| | R ≤ 0.7 mV | 1 |
| V5 [3] | Q ≥ 30 ms | 1 |
| | R/Q ≤ 1 | 2 |
| | R/S ≤ 1 | 2 |
| | R/Q ≤ 2 | 1 |
| | R/S ≤ 2 | 1 |
| | R ≤ 0.7 mV | 1 |
| V6 [3] | Q ≥ 30 ms | 1 |
| | R/Q ≤ 1 | 2 |
| | R/S ≤ 1 | 2 |
| | R/Q ≤ 3 | 1 |
| | R/S ≤ 3 | 1 |
| | R ≤ 0.6 mV | 1 |
| | **Total score:** | |

FIGURE 1.10 The 50-criteria, 31-point Selvester QRS scoring system. The panel shows the criteria and points for each lead. If 2 or more criteria are met within the same box, only the criterion that generates the highest number of points is considered. The maximum lead score is seen within parenthesis for each lead.

the precision of the standard ECG printout format when manually performing the scoring, Wagner et al.[43] determined the difference between using a standard printout format and a 4-fold magnified ("quad plot") format of the ECGs during manual QRS scoring. Their primary finding was that MI size can be systematically underestimated with use of the standard ECG printout format. The QRS scoring requires substantial time if individual ECGs are scored manually, but an automated version has been developed that is adequate for routine use.[42]

Except for QRS changes related to single MIs, the Selvester QRS scoring system is limited to ECGs with normal cardiac conduction; however, recently QRS scoring criteria for infarct quantification in the presence of cardiac conduction abnormalities have been suggested.[44] These criteria need further clinical validation. The presence of multiple MI may cause problems for QRS scoring; ECG changes due to both anterior and inferior MI might counterbalance each other and result in cancellation of QRS changes, and thus also of QRS criteria.[40]

The amplitudes and durations of QRS waveforms change with age and differ between sexes,[45] and the specificities of many of the criteria of the Selvester QRS scoring system have been shown to depend on age and sex,[38] variables that also affect its performance.[46] Age- and sex-specific QRS scoring criteria have been proposed, but these need further evaluation.[47]

## 1.4 Cardiac magnetic resonance imaging

Magnetic resonance imaging (MRI) is a noninvasive imaging technique, free of ionizing radiation, that uses a magnetic field and radio waves to acquire images of the human body. In MRI, different magnetic properties, such as water or fat content, of different tissues are used to obtain image contrast. Thus, this imaging technique has a unique ability to characterize soft tissues that makes it feasible for cardiac imaging. Its ability to acquire images in any arbitrary plane with no limiting acoustic windows has made cardiac MRI the refer-

ence method for noninvasive assessment of cardiac dimensions and function.

Cardiac MRI also has a unique ability to distinguish infarcted from noninfarcted myocardium noninvasively by use of the so-called "delayed-enhancement" technique.[48] By intravenous administration of an extracellular, gadolinium-based contrast agent 15–30 minutes before image acquisition, necrotic or scarred myocardium can be distinguished from viable myocardium. There is a relative increase in the amount of contrast agent in injured myocardium compared with viable myocardium, due an increase in regional fractional distribution of extracellular contrast media in the former.[49–52] The gadolinium-based contrast agent affects the surrounding tissue's magnetic properties, resulting in hyperenhancement of necrotic and scarred myocardium when applying a specific MRI acquisition sequence designed to enhance the contrast between viable and nonviable myocardium.[53]

Delayed enhancement-MRI (DE-MRI) has been shown to be a promising method for quantitative assessment of MI,[54,55] and is frequently used as a reference method to assess size and location of MI *in vivo*. Several aspects must be considered for accurate MI quantification, however, such as timing of imaging relative to the acute ischemic event,[56] contrast dose, time between injection of the contrast agent and image acquisition,[57] the relative contrast and brightness used in the image display, and how the delineation of the region of hyperenhancement is performed.[55] There is currently no international consensus regarding DE-MRI use for MI quantification.[58] Consequently, MI quantification can vary significantly between different laboratories and clinics.

## 1.5 Ischemic heart disease and myocardial infarction

In the Western world, ischemic heart disease (IHD) is a major cause of morbidity and mortality.[59] The term "ischemic" refers to insufficient blood supply relative to the demand of the tissues. The underlying cause of IHD is almost always atherosclerosis,[60] involving accu-

mulation of lipids and inflammatory cells, particularly in the inner layer (intima) of the arterial wall. Atherosclerosis principally occurs in medium-sized and large arteries such as the aorta and the coronary arteries,[61] and it can lead to the development of atherosclerotic plaques that protrude into the arterial lumen.[62] These may diminish or completely obliterate the lumen and thereby also reduce or completely block the blood flow. Angina pectoris appears when coronary blood flow cannot meet the demand of the cardiac muscle. Clinical manifestation of IHD depends on the extent of changes in the coronary arteries, the activity of the disease, and the function of the left ventricle. Stable coronary artery disease usually manifests as angina pectoris upon exertion, whereas unstable coronary disease can appear as unstable angina pectoris, acute MI, or sudden death. Heart failure is another clinical manifestation of IHD. This can develop as a consequence of myocardial cell death during MI or from chronic ischemia with fibrosis of the myocardium, so-called ischemic cardiomyopathy.

MI involves loss of heart muscle cells, local or regional cell death, and thus loss of electrically active myocardium. The underlying mechanism is rupture of an atherosclerotic plaque with subsequent coronary artery thrombosis (local clotting of the blood) and secondary effects on the myocardial blood supply. The delay until reperfusion therapy and its results are crucial determinants of the size of MI and thus the function of the heart. The presence of collateral vessels is also of importance for the size of MI.

Acute MI can be divided into 2 categories: ST-segment–elevation MI (STEMI), with typical ECG patterns involving elevation of the ST segment, and non-ST-segment–elevation MI (NSTEMI), which has more nonspecific ECG patterns. Acute chest pain occurring concurrently with ST-segment elevation indicates acute ischemia through the entire cardiac wall and impending MI, in most cases caused by a total occlusion of a coronary artery. Acute MI without ST elevation is, in most cases, a consequence of reduced myocardial perfusion caused by thrombosis that only partly occludes a coronary artery.[63] Serological biomarkers together with the patient's history, symptoms, and ECG, are important tools to diagnose acute MI. The aim of emergency

treatment of possible MI is to alleviate the pain, to limit the development of MI, and to reduce the risk for serious complications.

The ECG pattern of chronic MI can show more unspecific patterns, from normal appearance to reduced R-wave amplitudes and permanent Q waves.

## 1.6 ECG diagnoses mentioned in this thesis

### *Left- and right-axis deviation*

The left ventricle dominates the propagation of the electrical impulse through the ventricles, due to its thicker muscular wall compared with the right ventricle. Therefore the main direction in the frontal plane of propagation of the impulse through the ventricles (termed the electrical axis of the heart) is normally downwards and to the left, between 0° and +90° (Figure 1.3). An electrical axis < –30° is said to be deviated to the left, and an axis > +90° is said to be deviated to the right.

### *Left and right bundle branch block*

Normally the cells in the sinoatrial node generate the impulses, which thereafter propagate through the muscle cells of the right and left atria. In the cells of the atrioventricular (AV) node—the pathway between the atria and ventricles at the base of the right atrium—the propagation of impulses is relatively slow (because of the smaller size of these cells and fewer gap junctions compared with other myocardial cells); thus, the atria have time to contract before the ventricles are activated. From the AV node, the impulses propagate down the interventricular septum through the bundle of His. The bundle of His divides into a right bundle and a left bundle, which eventually leave the septum and enter the walls of the right and left ventricles, respectively. The right bundle continues in the right ventricle and branches off into Purkinje fibers, which are located below the endocardium and are the last branches of the conduction system. The left bundle divides into 1 anterior branch and 1 posterior branch called fascicles, which both also

branch off into Purkinje fibers. After the Purkinje fibers the impulses pass from cell to cell toward the epicardium.

Bundle branch block implies that the propagation of the impulse is blocked in either the left or right bundle, resulting in the impulse reaching the affected ventricle only by spread of excitation from cell to cell. Propagation of the impulse in the affected ventricle is outside the conduction system, which results in prolonged propagation time and a changed ECG appearance (prolonged QRS duration and ST–T-wave changes). Right-sided bundle branch block can indicate cardiac disease but also occurs among healthy individuals, whereas left-sided bundle branch block almost always indicates cardiac disease.

### *Left and right atrial enlargement*

Enlargement of the left atrium can be due to diseases of the mitral valve. When this atrium is enlarged, the spread of the rhythmic impulses through its myocardium takes longer time than usual, so the P-wave duration in the ECG is increased.

Enlargement of the right atrium is often due to chronic pulmonary disease. In normal circumstances, rhythmic impulses first spread through the myocardium of the right atrium. Thus in right atrial enlargement with an enlarged P vector, the first part of the P-wave amplitude in the ECG is increased.

However, the ECG is a nonspecific and insensitive method for diagnosing atrial enlargement.

### *Left and right ventricular hypertrophy*

Left ventricular hypertrophy can reflect prolonged, untreated hypertension, stenosis of the aortic valve, or other disorders. Left ventricular hypertrophy results in large vectors directed to the left, that is, increased R-wave amplitudes in the left-sided ECG leads, increased S-wave amplitudes in right-sided ECG leads, and often left-axis deviation. The spread of excitation through the myocardium takes longer than usual, which can result in a prolonged QRS complex duration. ST–T-wave changes often develop in the left-sided ECG leads.

Right ventricular hypertrophy can result from congenital heart disorders such as stenosis of the pulmonary valve, or to chronic lung diseases that cause increased pressure in the pulmonary circulation. Hypertrophy of the right ventricle results in larger vectors directed to the right, that is, increased R-wave amplitudes in the right-sided ECG leads, increased S-wave amplitudes in the left-sided ECG leads, and often right-axis deviation. ST–T-wave changes can be seen in the right-sided ECG leads. Hypertrophy of the right ventricle must be fairly pronounced for it to be evident in the ECG.

The ECG is a nonspecific and insensitive method for diagnosing ventricular hypertrophy.

# 2 Aims of the Thesis

The first aim of this thesis was to further validate the EASI lead system to gain more knowledge about the agreement between EASI-derived and standard 12-lead ECGs. The second aim was to investigate the possibility of optimizing the positions of proximally placed limb electrodes for standard 12-lead ECGs.

The specific aims for each paper were:

*Paper I*; to 1) simultaneously collect standard 12-lead ECGs and ECGs using EASI electrode positions in children of various ages, 2) develop and determine the value of using age-specific transformation coefficients for deriving 12-lead ECGs, and 3) study the "goodness-of-fit" between the standard and derived 12-lead ECGs.

*Paper II*; to compare the intrareader variation in interpretation of standard 12-lead ECGs with the variation in interpretations of standard vs. EASI-derived 12-lead ECGs in children.

*Paper III*; to test the hypothesis that the EASI lead system is less susceptible to baseline wander and myoelectric noise than is the M-L lead system.

*Paper IV*; to 1) compare the differences in Selvester scores for chronic MI provided from standard and EASI-derived 12-lead ECGs, and 2) compare these scores with MI sizes as measured by DE-MRI.

*Paper V*; to test the hypotheses that 1) compared with the M-L lead system, the LU lead system produces ECG waveforms with closer relationship to the morphologies of the waveforms obtained from the standard lead system with regard to the QRS axis in the frontal plane and QRS-estimated inferior MI size, and that 2) the LU lead system is more noise-immune than the standard lead system, and that 3) the noise immunities of the LU and M-L lead systems are comparable.

# 3 Materials and Methods

## 3.1 Study populations

*Paper I and Paper II*: Two hundred and twenty-one children of various ages, healthy and with varying cardiac diagnoses, admitted to the Department of Pediatric Cardiology at the Lund University Hospital, Lund, Sweden were included in these studies. The protocols were approved by the Ethics Committee at Lund University, and informed consent was given by the parent/guardian or the individual, depending on age.

*Paper III*: Nineteen healthy volunteers, all staff at the Department of Clinical Physiology, Lund University Hospital, were included in this study. The protocol was approved by the Ethics Committee at Lund University. Informed consent was given by the volunteers.

*Paper IV*: Thirty-seven individuals enrolled in the MRACS (Magnetic Resonance in Acute Coronary Syndromes) study at the Glasgow Western Infirmary[64] were included in this sub-study. The study complied with the Declaration of Helsinki. The protocol was approved by the Ethics Committee of the North Glasgow University Hospitals NHS Trust. Written informed consent was given by the individuals.

*Paper V*: Eighty patients, women and men, with normal waveform morphologies, left QRS axis deviation, or QRS changes of inferior MI in their standard ECGs were included for the primary aim of the study. The infarcts were identified by significant inferior Q waves or Q-equivalent patterns according to the Glasgow ECG interpretation program.[65,66] The other ECGs were also interpreted by this program. The noise-immunity sub-study included 11 patients from the original cohort and 9 healthy volunteers. All patients were admitted to the Lund University Hospital, either to the Department of Clinical Physiology, the Cardiac Intensive Care Unit, or the Medical Emergency Care Unit.

The healthy volunteers were enrolled at the Department of Clinical Physiology. The Ethics Committee at Lund University made an advisory statement in which the study was considered to be valuable, and there were no objections against it from an ethics point of view.

## 3.2 ECG acquisition and analysis

### Papers I and II

In each individual, the standard 12-lead and the EASI ECGs were acquired simultaneously at rest, with the individuals in supine position, using a PageWriter XLi (Philips Medical, Oxnard, CA) during 10 seconds. The same ground electrode was used for both lead systems. The sampling rate was 500 samples/s, and the amplitude resolution was 5 µV. The ECG signals were saved in digital format on a computer diskette for further processing offline. Each lead of the derived 12-lead ECG was constructed by linear combination of the 3 bipolar ECG leads of the EASI system: AI, ES, and AS (for example, derived V2 = a*AI+b*ES+c*AS).

In *Paper I*, the optimum coefficients (a, b, and c) were calculated for each lead and each age group (< 1 year, 1–6 years, 7–12 years, and 13–18 years) that minimized the aggregate root-mean-square (RMS) difference between the standard and EASI-derived 12-lead ECGs. RMS denotes the square root of the mean value of the squared differences. RMS differences were computed starting at the onset of the QRS complex and ending at the end of the T wave. The resulting RMS difference expressed the "goodness-of-fit," that is, the similarity of the 2 sets of waveforms. The results of using age-specific coefficients were compared with the results of using coefficients developed for adults.

In *Paper II*, the age-specific transfer coefficients calculated in *Paper I* were used when deriving the 12-lead ECGs from the EASI lead system. The printouts of the ECGs did not indicate which lead system was used, and all ECGs were submitted to the readers in random order. Two experienced pediatric cardiologists interpreted the ECGs.

The readers used structured case report forms in which they were asked to make an overall assessment and to assess and report the rhythm, the electrical axis (mean vector) in the frontal plane, the presence of possible bundle branch block, and the presence of possible abnormality of the atria or hypertrophy of the ventricles. First, each reader interpreted a set of 221 ECGs with randomly allocated standard and EASI-derived 12-lead ECGs. Next, the readers interpreted the complementary ECG set without having access to the first set. Finally, the readers reinterpreted the standard ECGs from 98 children.

## *Paper III*

In each individual, the M-L and the EASI ECGs were simultaneously acquired at rest during 10 seconds, with the individuals in supine position, and during the performance of 5 different physical activities, using a PageWriter XLi (Philips Medical, Oxnard, CA). The sampling rate was 500 samples/s, and the amplitude resolution was 5 µV. The ECG signals were stored digitally for later offline processing. The same ground electrode was used for both lead systems. Each lead of the derived 12-lead ECG was constructed by linear combination of the 3 bipolar ECG leads of the EASI system using optimal transfer coefficients.[14]

For each lead in each individual, the baseline wander and the myoelectric noise amplitudes were calculated and compared at rest and during each physical activity for both lead systems (Figure 3.1). Baseline wander (low-frequency noise; $\leq$ 1–2 Hz) was quantified by fitting a regression model to the original ECG signal with use of a regularized least-square criterion.[67] Baseline wander was defined as the peak-to-peak amplitude of the estimated baseline during the 10-s recording. Myoelectric noise primarily contains frequency components > 15 Hz. We therefore quantified noise after the signal had been high-pass filtered (filter cutoff frequency, 15 Hz) and the QRS complexes had been blanked. The RMS value was computed in each R–R interval of the processed signal, and the largest value was taken as the measurement of myoelectric noise for that record.
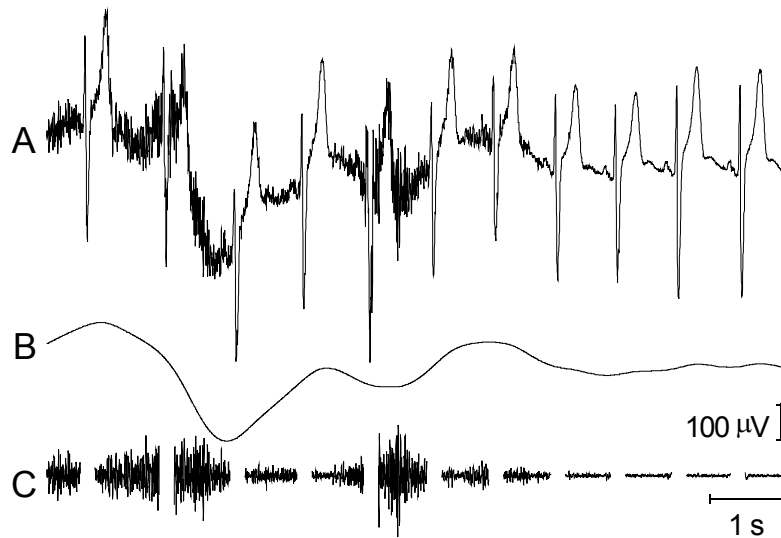
FIGURE 3.1 A, Original 10-s epoch in a precordial lead during a change in body position. B, Estimated baseline wander during the epoch. C, Filtered-out myoelectric noise during the epoch. A segment around and including each QRS complex has been blanked.

If the difference in the measurements between the M-L and EASI systems was < 25 µV for myoelectric noise or < 300 µV for baseline wander, the results were declared "equal" for the 2 systems. These 2 threshold values were selected with reference to a signal amplitude at which the noise begins to have a clinical impact on the ECG interpretation. If the difference was greater than these respective thresholds, a "winner" was declared.

## Paper IV

For each patient, BSPM was made with 120 electrodes placed in a standardized way[68] at rest with the subject in supine position during 15 seconds. The sampling rate was 1000 samples/s, and the amplitude resolution was 1 µV. Data processing was performed offline. The averaged PQRST waveforms from the standard 12-lead and the EASI ECG leads were extracted from the BSPM data. Thus, the standard 12-lead and the EASI ECGs were simultaneously acquired. Each lead of the derived 12-lead ECG was constructed by linear combination of the 3 bipolar ECG leads of the EASI system using optimal transfer coefficients for adults.[14] The standard and the EASI-derived 12-lead ECGs were printed in a quad plot format,[43] which magnifies the ECG waveforms 4-fold along each axis (100 mm/s and 40 mm/mV compared with the conventional scale; 25 mm/s and 10 mm/mV) as illustrated in Figure 3.2. The quad plot format facilitates quantitative ECG measurements by allowing the waveforms to be viewed more clearly and measured more precisely. Selvester QRS scoring[40] was performed for all patients.

## Paper V

For each of the 80 patients in the morphology study, 2 standard, 1 LU, and 1 M-L 12-lead ECGs were recorded within a few minutes of each other, at rest with the patient in supine position. The positions of the distal limb electrodes were unchanged between the 2 standard recordings. For both alternative lead systems, the precordial electrodes remained in the same positions as for the standard 12-lead ECG. For each of the 20 individuals in the noise-immunity sub-study, 2 standard, 2 LU, and 2 M-L ECGs were recorded in sequence while the individuals, in supine position, performed 2 different limb movements known to influence the technical quality of the ECG signal. The individuals began the movements a few seconds before the 10-s ECG recording began, to ensure that noise generated by the limb movements would be present in the analyzed ECG.

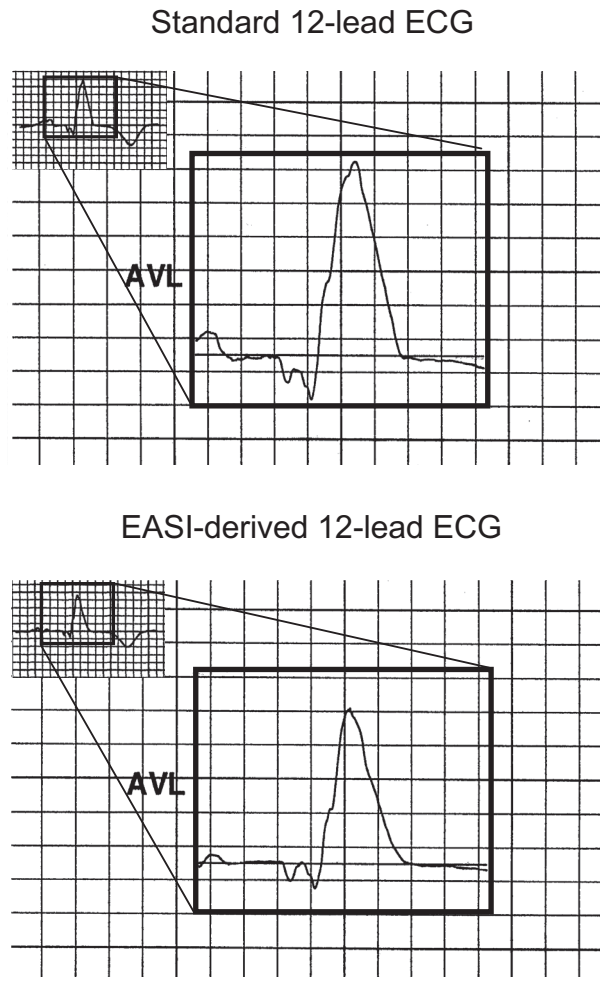## Standard 12-lead ECG



## EASI-derived 12-lead ECG



FIGURE 3.2 Example of the quad plot format compared with the conventional format for the standard 12-lead ECG (top) and the EASI-derived 12-lead ECG (bottom). The small complex illustrates the conventional format, 25 mm/s and 10 mm/mV, and the large complex illustrates the quad plot format, 100 mm/s and 40 mm/mV.

The recordings were made either with a Megacart recording device (Siemens-Elema AB, Solna Sweden) or with a MAC 5500 recording device (GE Healthcare, Milwaukee, WI, USA). In both recording devices, the ECG signals were stored with a sampling interval of 2 ms.

In the morphology study, all ECGs were reanalyzed in the Infinity Megacare ECG server (Draeger Medical, Telford, PA, USA), which uses a Draeger version (#24), of the Glasgow program[65,66] to process the ECGs. For all 80 patients, we chose the QRS axis in the frontal plane for comparative analysis. We performed Selvester scoring[40] for all patients except for those 5 who had ECG findings considered confounding factors for QRS scoring (left ventricular hypertrophy, or left anterior fascicular block). One patient who had QRS changes of anterior MI, and 1 patient who had QRS changes of multiple MI were also excluded. The differences in measurements between standard and LU ECGs, and between standard and M-L ECGs, were compared with the differences between the 2 standard ECGs. For each patient, the first standard 12-lead ECG was used as the "gold standard" for comparison with all the other ECGs.

Three ECG readers subjectively assessed the noise immunity in each of the 6 ECGs obtained from each of the 20 individuals. The printouts of the ECGs did not indicate which lead system was used, and the ECGs were submitted to the readers in random order. The readers used a scale of 1 through 5 to indicate how much they thought the limb movements influenced the technical quality of the ECG signal, with 1 = very little influence, 2 = little influence, 3 = moderate influence, 4 = pronounced influence, and 5 = very pronounced influence. The readers assessed the total noise influence from the limb movements, both myoelectric noise from muscle activity and baseline wander from variations in electrode impedance caused by the physical activity. Influence levels 1 and 2 were combined for analysis, as were influence levels 3–5, because we assumed that influence levels 1 and 2 should not influence diagnostic accuracy, whereas influence levels 3–5 might. When evaluating the data, the assessments from the 3 readers were combined.

## 3.3 Infarct quantification by the Selvester QRS scoring system

*Papers IV and V*

Figure 1.10 shows the 50-criteria, 31-point Selvester QRS scoring system[41] used in both papers. As mentioned in the introduction section (1.3), each point represents infarction of approximately 3% of the left ventricle. For example, in lead I, QRS points can be awarded for the Q-wave duration, the R-wave amplitude, and the R/Q-amplitude ratio. If the Q wave is $\geq 30$ ms, 1 point is awarded, and if the R/Q-amplitude ratio is $\leq 1$ and/or the R-wave amplitude is $\leq 0.2$ mV, 1 additional point is awarded.

In Paper IV, 2 investigators, independent of each other and blinded to the MRI results, manually measured the QRS waveforms required for Selvester QRS scoring. Differences in Selvester scores provided from EASI-derived versus standard 12-lead ECGs were compared with the intrareader variation (for 1 of the investigators) in Selvester scores for the standard 12-lead ECGs. Differences in points between the 2 observers were assessed in conference for comparison with the MRI results. The results from the 2 lead systems were systematically compared with the cardiac MRI results.

In Paper V, The Selvester scoring was based upon the Glasgow program waveform measurements, and calculated by 1 of the authors (AW). Another author (OP) scrutinized QRS morphologies and the automated measurements to possibly discover any mismeasurements of waveforms. A third author (GW) performed Selvester scoring based on visual/manual measurements. The group of investigators determined "adjudicated" scores in conference. No QRS measurements were changed in this process, but some Selvester cores were. The scores from the 48 patients without QRS changes of MI were evaluated as were also the scores from the 25 patients with QRS changes of inferior MI. The final score was only counted if the ECG complied with the screening criteria of Anderson et al.[69]

## 3.4 Infarct quantification by DE-MRI

*Paper IV*

Cardiac MRI was performed on a 1.5-Tesla whole-body scanner (Magneton Sonata, Siemens AG, Erlangen, Germany) with a phased-array chest coil. The images were acquired with the patients lying in supine position during breath hold. Image acquisition was gated to the ECG. For the measurement of left ventricular dimensions and function, a short-axis cinematographic (CINE) stack of the left ventricle was acquired. For infarct quantification, DE-MRI was performed in corresponding short-axis slices using the standard segmented gradient-echo inversion-recovery sequence as described elsewhere.[53] Measurement of the left ventricular mass was evaluated using manual planimetry on commercially available Argus software (Siemens, Erlangen, Germany) by an observer blinded to all other clinical data. The DE-MRI data were analyzed using CMR Tools (Imperial College, London, UK). Regions of MI by DE-MRI were defined as those with hyperenhancement involving at least the subendocardium. The epi- and endocardium were manually delineated with computer-assisted planimetry, and the signal intensities of gadolinium-enhanced myocardium were also manually delineated.

## 3.5 Statistical analysis

*Paper I*

The paired t-test was used to test differences between RMS values based on adult and age-specific coefficients for each ECG lead.

*Paper II*

The agreement between interpretations of standard and EASI-derived 12-lead ECGs was evaluated with the kappa ($\kappa$) statistic,[70] a measure of how much better the agreement between the interpretations is than what could be expected by chance. Student's t-test was used to com-

pare the κ value for the agreement between standard and EASI-derived 12-lead ECGs with the κ value for the intrareader agreement of standard 12-lead ECGs.

### Paper III

The $\chi^2$ statistic was used to compare the proportion of winners in the EASI and M-L lead placement groups. In situations where there were no winners in 1 of the 2 groups, Fisher's exact test was used. One *P* value was determined for the summed limb leads and the summed precordial leads for each physical activity separately.

### Paper IV

The Spearman rank correlation coefficient was used to assess the correlation between MI size estimated from the standard and EASI leads, from EASI leads and MRI, and from standard leads and MRI. The Bland-Altman method,[71] was used to evaluate the agreement in MI size estimates between the 2 lead systems. Within-individual differences between the various methods were compared with the Wilcoxon signed-rank test.

### Paper V

The paired t-test was used for comparison of the QRS axis variables obtained with each method; the Wilcoxon signed-rank test was used for the MI size variables, and the $\chi^2$ statistic was used to compare categories of the noise-immunity variables.

# 4 Results and Comments

## 4.1 Comparison of waveforms and diagnostic conclusions from EASI and standard ECGs in children (Papers I and II)

RMS differences decreased with increasing age. In the subgroup of adolescents 13–18 years of age, the RMS difference using the age-specific coefficients was very similar to that obtained in adults (Figure 4.1). Comparison of the RMS differences showed that the age-specific coefficients typically yielded between 10% and 16% lower RMS differences than did the adult coefficients.
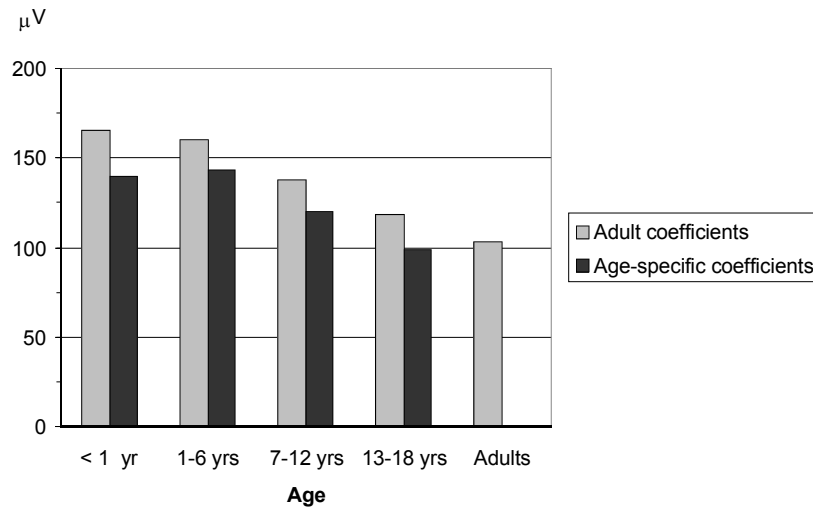


FIGURE 4.1 RMS differences between EASI-derived and standard 12-lead ECG waveforms, averaged over all 12 leads, as observed in the four pediatric age groups and in an adult population. The result of using age-specific versus adult coefficients is compared.

For each age group, the largest RMS differences were observed in either lead V2 or V4. The smallest RMS difference was found in lead V6 in each age group.

The RMS differences obtained using the age-specific coefficients were only slightly larger than those previously found in a set of ECGs from adults, and the overall goodness-of-fit expressed as RMS differences was similar to that reported in adults (D. Field, Philips Medical Inc; personal communication).

When the possibilities for interpretation by the readers were several categories (e.g. hypertrophy of the right or left ventricle was categorized as none, possible, probable, or definite), there was a considerable intrareader variation in the interpretation of standard 12-lead ECGs for both readers, as reflected by the κ values, and the variation in the interpretation of EASI-derived versus standard 12-lead ECGs was only slightly larger (Table 4.1). Furthermore, for most of the ECG diagnoses, for both readers, the differences in agreements between the EASI-derived and the standard 12-lead ECGs were not statistically significant.

When the possibilities for interpretation by the readers were reduced to 2 categories, normal and abnormal (that is, all other classes combined), the intrareader agreement still varied considerably in the interpretation of standard 12-lead ECGs. The differences in agreements between the EASI-derived and standard 12-lead ECGs did not achieve significance for any of the ECG diagnoses.

The algebraic transfer coefficients that were used to derive the 12-lead ECG from the EASI leads were based on the QRST waves and not on the P waves; thus, the EASI derivation might tend to influence P wave morphology and assessment of the rhythm more than QRST wave morphology. For both readers, the agreement for ventricular hypertrophy was better than that for atrial abnormality when comparing EASI versus standard. The EASI lead system, on average, causes a shift of the direction of the electrical axis in the frontal plane,[22] and, as expected, the intrareader agreement for axis deviation was better than the agreement between EASI-derived and standard 12-lead ECGs.

TABLE 4.1 Intraobserver agreements (κ) in EASI versus standard ECG and standard ECG 1 versus standard ECG 2, and differences in these agreements (*P* values).

| | | Right atrial abnormality | Left atrial abnormality | Right ventricular hypertrophy | Left ventricular hypertrophy | Bundle-branch block | Sinus rhythm | Axis deviation | Final interpre-tation |
|---|---|---|---|---|---|---|---|---|---|
| Reader 1 | EASI vs. stan-dard | 0.30 | 0.22 | 0.60 | 0.54 | 0.68 | 0.91 | 0.60 | 0.62 |
| | Standard 1 vs. standard 2 | 0.51 | 0.30 | 0.65 | 0.33 | 0.79 | 1.00 | 0.80 | 0.76 |
| | *P* value | 0.20 | 0.59 | 0.54 | 0.22 | 0.30 | —* | 0.016 | 0.006 |
| Reader 2 | EASI vs. stan-dard | 0.30 | 0.13 | 0.43 | 0.38 | 0.67 | 0.45 | 0.58 | 0.43 |
| | Standard 1 vs. standard 2 | 0.30 | 0.06 | 0.59 | 0.34 | 0.72 | 0.73 | 0.82 | 0.47 |
| | *P* value | 0.99 | 0.22 | 0.048 | 0.73 | 0.76 | 0.12 | 0.14 | 0.60 |

* Cannot be calculated because of perfect agreement between standard 1 and standard 2.

There was considerable intrareader variability for several of the ECG diagnoses. Other ECG studies with less intrareader variability have been reported.[72,73] The larger κ values found in those studies could at least partly be explained by the fact that those ECGs were from adults and that the studies focused on measurements of amplitude and duration rather than on interpretations.

*Papers I* and *II* showed that the age-specific transformation coefficients performed slightly better than the adult coefficients did and that the agreement of the waveforms between the standard and EASI systems was mostly good. Furthermore, the variation in the interpretation of standard versus EASI ECGs was only slightly larger than the intrareader variation in the interpretation of standard ECGs.

## 4.2 Noise immunity of the EASI lead system and its capacity to predict MI size (Papers III and IV)

### *Baseline wander*

We found few differences between the EASI and M-L systems either at rest or during physical activities required for "arms up" or cycling. The EASI lead system was superior, attaining a significantly higher number of "wins" in the precordial leads, for treadmill exercise and for turning supine-to-left (Figure 4.2), whereas the M-L system attained a significantly higher number of wins for turning supine-to-right in both the limb and the precordial leads.

### *Myoelectical noice*

We found few differences between EASI and M-L either at rest or during physical activities required for arms up, whereas the EASI lead system was superior, attaining a significantly higher number of wins in the limb leads for treadmill exercise, cycling, and for turning supine-to-left (Figure 4.3). However, M-L attained a significantly higher number of wins in the precordial leads for turning supine-to-right.

EASI is much more susceptible to both baseline wander and myoelectrical noise than is M-L when turning from supine to the right

side, because only the EASI lead system uses an electrode placed in the right-midaxillary line. Overall, however, the M-L and the EASI lead systems did not show large differences regarding susceptibility to baseline wander, most likely because variations in electrode impedance, the primary cause of baseline wander, affect the electrodes of the 2 systems equally, and EASI is less susceptible to myoelectrical noise than is M-L.
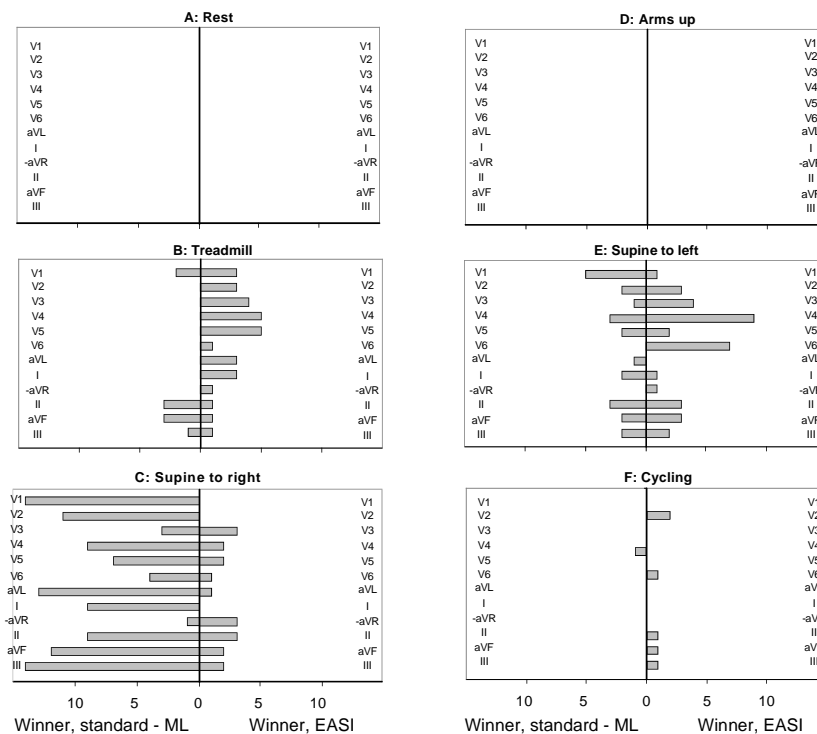


**Baseline wander**

FIGURE 4.2 Comparison of the outcomes with the M-L and EASI lead systems for baseline wander at rest (A) and during all five physical activities (B–F). On the horizontal axis, the "0" indicates equivalent performance of the M-L and EASI-derived 12-lead ECGs. A longer bar to the right than to the left indicates superiority of EASI, and vice versa. The numbers on the horizontal axis indicate the frequency of these occurrences.
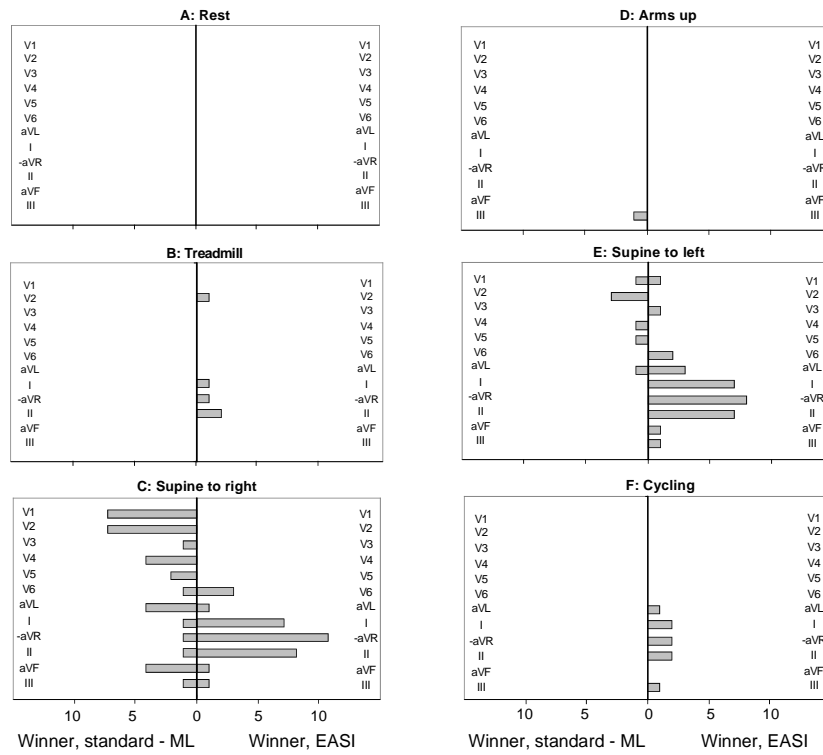
**Myoelectrical noise**



FIGURE 4.3 Comparison of the outcomes with the M-L and EASI lead systems for myoelectric noise at rest (A) and during all five physical activities (B–F). The same conventions apply as described in Figure 4.2.

## *Estimated infarct size*

The EASI lead system often gave higher Selvester scores and thereby estimated the MI to represent a larger percentage of the left ventricle than did the standard lead system (Figure 4.4). The mean difference in the percentage of infarcted left ventricle between standard and EASI systems was −1.4% ± 4.3%. The agreement between the 2 lead systems can be less than satisfactory at times, but the difference between the intrareader variation in Selvester scores for standard ECGs and the variation between the EASI and standard ECGs was not statistically significant ($P = 0.26$).
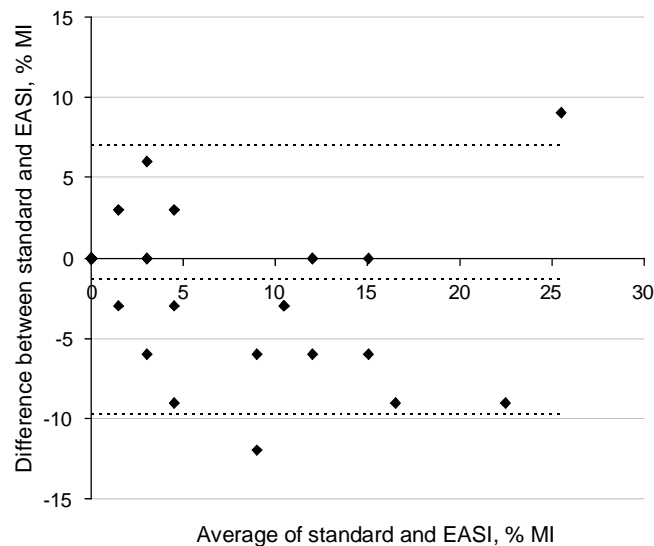
FIGURE 4.4 Bland-Altman plot for MI size, as indicated by percent of the myocardium affected, for standard vs. EASI-derived 12-lead ECGs. The X axis represents the average percentage of infarcted myocardium of the standard and EASI-derived 12-lead ECGs. The broken line just below the X axis represents the mean difference in the percentage of infarcted myocardium between the 2 lead systems for all patients, and the 2 outer broken lines represent 2 standard deviations from this mean difference. The Y axis represents the difference in percentage of infarcted myocardium between the 2 lead systems.

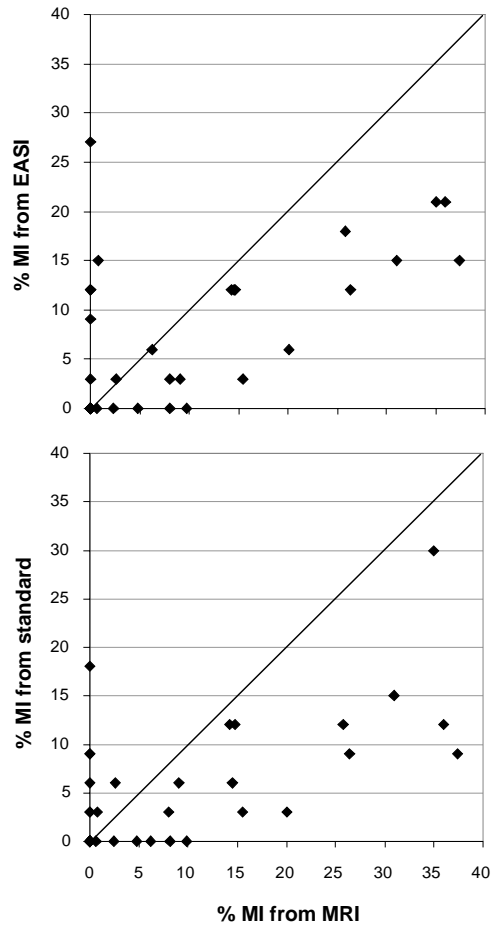FIGURE 4.5 Relationship for infarct size, expressed as percentage of the left ventricle affected, between MRI measurements and the EASI lead system (top) and between MRI measurements and the standard lead system (bottom). The line in the diagrams is the identity line. Neither the correlation nor the agreement between MI sizes estimates by Selvester scores from both of the 2 lead systems and by MRI were very strong.

The 2 ECG lead systems often underestimated the percentage of infarcted left ventricle compared with cardiac MRI, and both lead systems missed MI in several cases and had false-positive MI results compared with imaging (Figure 4.5). The mean difference in the percentage of infarcted left ventricle between MRI and EASI 12-lead ECGs was 2.6% ± 9.5%; between MRI and the standard 12-lead ECGs, it was 3.6% ± 9.0%. The agreement between MRI and each lead system can differ considerably in individual cases. The difference in variations between MRI and the EASI system versus the variations between MRI and the standard system was not statistically significant ($P = 0.08$).

*Paper III* showed that, overall the 2 lead systems have similar susceptibilities to baseline wander. However, the EASI lead system is less susceptible to myoelectric noise than is the M-L lead system.

*Paper IV* showed that the estimations of MRI-measured MI size of standard and EASI-derived 12-lead ECGs were comparable. Neither the correlation nor the agreement between ECG and MRI measurements of MI size were very strong.

### *Update since publication of Paper IV*

There is no international consensus for MI quantification by cardiac MRI. Thus, differences in measured MI size between laboratories can be significant.

After *Paper IV* was published, the MRI data were reevaluated by means of a recently validated MI quantification method.[55] The original Glasgow MRI measurements of infarct size were, on average, 51% larger than the measurements of the validated method (Figure 4.6).

When the MRI measurements of the validated method are compared with ECG-estimated MI sizes, the concordance between the ECG and MRI methods is markedly improved (Figure 4.7).
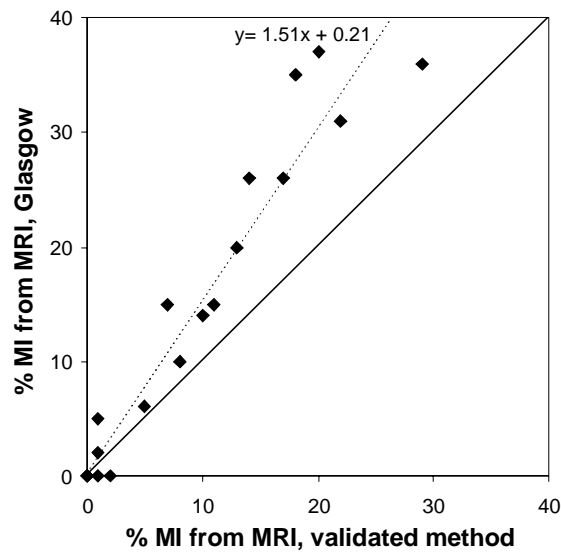
FIGURE 4.6 Relationship for infarct size, expressed as percentage of the left ventricle affected, between the validated method and Glasgow MRI measurements. The whole line in the diagram is the identity line, and the broken line in the diagram is the regression line. The equation is the equation for the regression line.
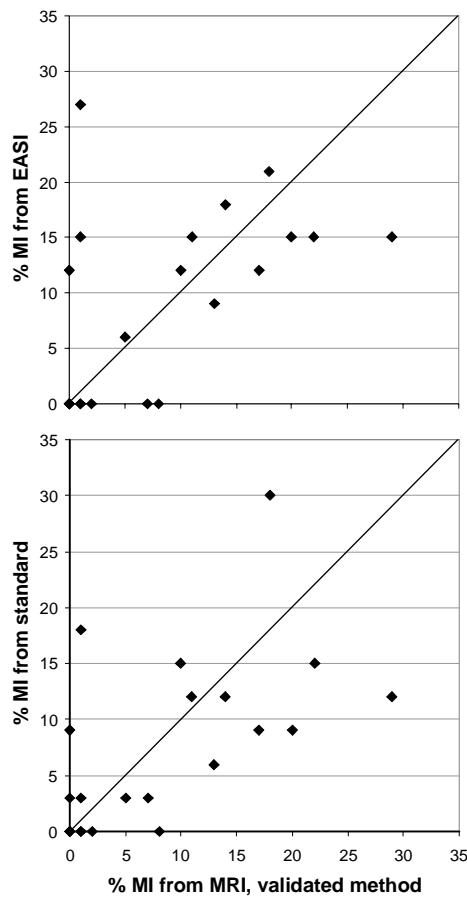
FIGURE 4.7 Relationship for infarct size, expressed as a percentage of the left ventricle affected, between MRI measurements of the validated method and the EASI system (top) and between MRI measurements of the validated method and the standard system (bottom). The line in the diagrams is the identity line.

The new MI quantification method is based on an automated computer algorithm that accounts for partial-volume effects in the quantification process. This method has been validated in computer phantoms, in animals, and in humans.[55] The Glasgow MI measurements were performed manually, not taking partial-volume effects into account.

## 4.3 12-lead ECG waveforms from monitoring positions (Paper V)

Variability in QRS axis between the 2 standard ECG recordings was compared with standard vs. LU as well as standard vs. M-L (Figure 4.8). The analysis included all 80 patients to provide a wide range of QRS axes. Most of the patients with the QRS axis within normal limits, $\geq -30$ degrees and $\leq 90$ degrees, in their standard ECGs had a marked rightward QRS axis shift (mean difference 22 degrees) in their M-L ECGs. A small rightward QRS axis shift (mean difference 4 degrees) was also seen in most of the corresponding LU ECGs. The axis shifts were statistically significant ($p < 0.0001$), but the difference in QRS axis between the standard and LU ECGs should have little clinical importance.

When analysing the Selvester scores calculated from the 48 patients without QRS changes of MI, only 3 patients received scores. One received scores in the first standard ECG recording only, 1 in both the second standard and in the LU ECG recordings, and 1 in both the standard and in the LU ECG recordings. There were no scores in the M-L ECG recordings.

Variability in Selvester scores between the 2 standard ECG recordings was compared with standard vs. LU as well as standard vs. M-L (Figure 4.9). The analysis included all 25 patients with QRS changes of inferior MI. Compared with the first standard ECG, there were both false-positive and false-negative diagnoses in the second standard ECG and in the LU ECG, and false-negative diagnoses in the M-L ECG. The difference in estimated infarct size between standard and M-L recordings was statistically significant ($p = 0.008$), but the difference between standard and LU was not ($p = 0.72$).
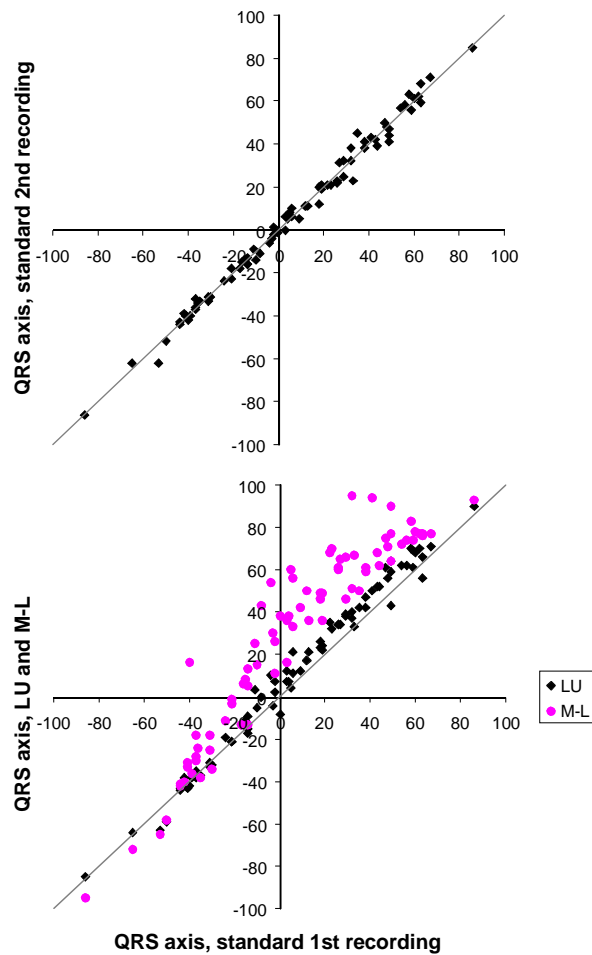
FIGURE 4.8 Relationships for the QRS axis between the first and second standard ECG recordings (top) and between the first standard and the LU and M-L ECG recordings (bottom), for each of the 80 patients. The line in each diagram is the identity line.
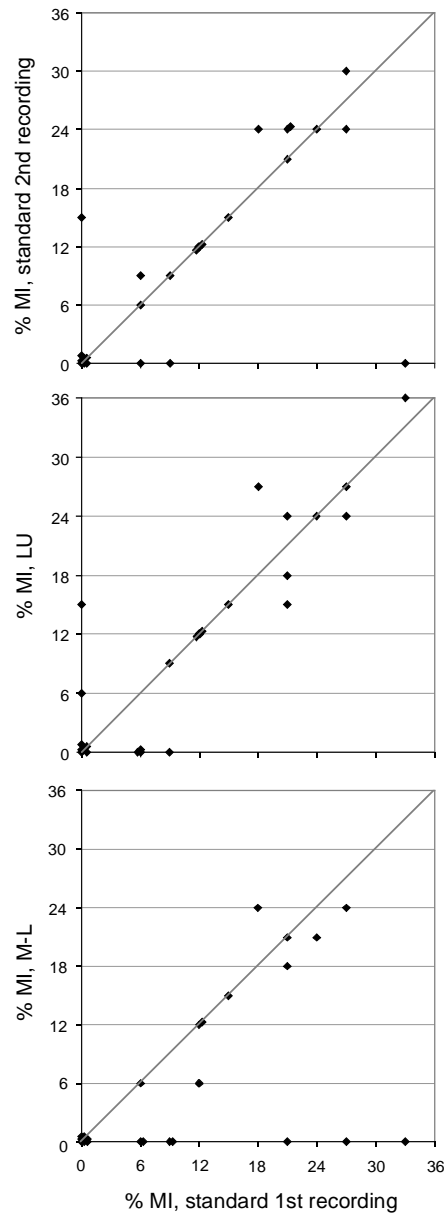
FIGURE 4.9 Relationship between the first and second standard ECG recordings (top), between the first standard and the LU ECG recordings (middle), and between the first standard and the M-L ECG recordings (bottom) for infarct size expressed as percentage of the left ventricle, for each patient with QRS changes of inferior MI. The numbers of patients at the origin are 7 in the top diagram, 6 in the middle diagram, and 8 in the bottom diagram. The numbers of patients on the x-axis are 3 in the top diagram, 4 in the middle diagram, and 7 in the bottom diagram. The line in each diagram is the identity line.

The difference in noise immunity between standard, LU and M-L ECG recordings was compared with regard to arm and leg movements (Figure 4.10). The difference between standard and LU was statistically significant for both arm and leg movements (both comparisons, $p < 0.0001$). The difference leg vs. arm movements was statistically significant for M-L ($p = 0.028$), but not for LU ($p = 0.087$). The difference between M-L and LU was not statistically significant, neither for arm movements ($p = 0.25$) nor for leg movements ($p = 0.10$).
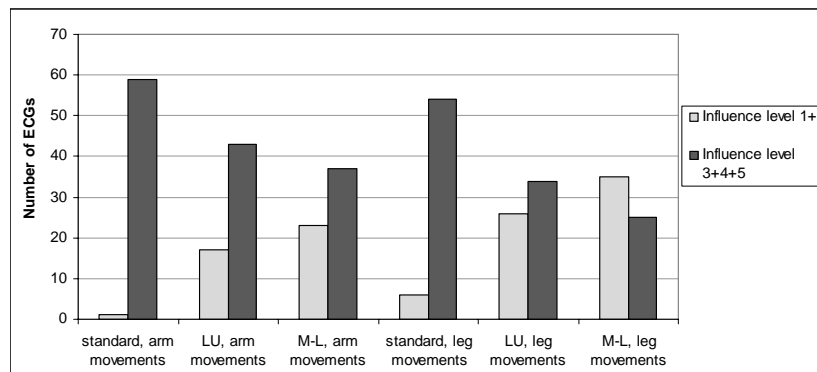


FIGURE 4.10 Noise immunity of the standard, LU, and M-L lead-placement systems.

The study results confirm our hypothesis that, with regard to the QRS axis in the frontal plane and inferior MI size, the LU electrode-placement system produces ECG waveforms that more closely resemble the waveforms obtained with the standard ECG than does the M-L electrode-placement system. Furthermore, the LU system is more noise immune than the standard system, and the noise immunities of the LU and the M-L systems are comparable.

## 4.4 Limitations of the studies

### Papers I and II

Age was taken into account in both *Paper I* and *Paper II*. Weight and height, though dependent on age, might have contributed to better agreement of the derived ECG with the standard tracing, but this was not specifically investigated.

The RMS difference used in *Paper I* is the most commonly used method for comparing waveforms, but it can be a crude way of expressing similarities or finding differences between detailed waveform patterns.

In *Paper II*, the reader knew the exact age for patients <1 year old only when he had specifically asked for it. There could have been cases for which the interpretation would have improved if more detailed information on age had been given for each patient in this age group.

### Paper III

Some common artifact-generating movements that can cause false alarms, such as combing hair, brushing teeth, and shaving, were not included in the protocol.

The subjects were all relatively young (30–64 years) and healthy, which is not representative of the population monitored in hospitals. Myoelectrical noise and baseline wander might be influenced by age and infirmity.

### Paper IV

The small study population could explain the lack of significance for the difference between the intrareader variation in Selvester scores for standard 12-lead ECGs versus the variation between EASI-derived and standard 12-lead ECGs.

The investigators had access only to the average complexes of the ECGs. When it was difficult to be certain of the beginning of the QRS

complex, it might have been valuable to have access to the complete ECG signal.

For 8 of the 37 patients, there was a delay (4−340 days) between the BSPM and the cardiac MRI scanning, with the BSPM being made after MRI.

The MRI is used as the gold standard for quantification of MI, although there is no international consensus on the parameters required for accurate MI visualization and sizing by cardiac MRI.[58] As a result, there could be large differences in MI size between laboratories and clinics.

## *Paper V*

The subgroups were rather small, and only a few aspects of ECG morphology were investigated. However, we chose the variables to be studied based on where the largest influence on the ECG waveforms could be expected when moving electrodes from the standard positions to the torso.

The best way of evaluating possible differences between the lead systems would have been to simultaneously record the 4 ECGs for each patient. Because this was not possible, all ECGs were recorded in direct sequence.

In real situations, movements other than those studied are of course also performed, and no data exist to establish the validity of the 5-point scale used to assess the influence of limb movements on the technical quality of the ECG signal.

# 5 Major Conclusions

The major conclusions of each paper were that:

I. EASI leads in children have the same high level of "goodness-of-fit" to replicate standard 12-lead ECG waveforms, as reported earlier in adults.

II. For most of the ECG diagnoses, similar diagnostic conclusions can be achieved from EASI-derived and standard 12-lead ECGs, supporting the suggestion that the EASI lead system is a potential alternative to standard lead placement in children.

III. The EASI and the M-L lead systems have similar susceptibilities to baseline wander. However, the EASI lead system is less susceptible to myoelectric noise than is the M-L system.

IV. The estimations of MRI-measured MI size of standard and EASI-derived 12-lead ECGs were comparable. The agreement between ECG and MRI measurements of MI size was only moderate.*

V. Compared with the M-L electrode-placement system, the LU electrode-placement system produces ECG waveforms that more closely resemble the waveforms obtained with the standard ECG. The LU system is more noise immune than the standard system, and the noise immunities of the LU and M-L systems are comparable.

*MI sizes measured by MRI have since been remeasured by means of a recently validated MI quantification method.[55] When the MRI measurements of the validated method were compared with the ECG-estimated MI sizes, the agreement between the ECG and MRI methods was markedly improved.

# References

1. Waller A. A demonstration on man of electromotive changes accompanying the heart's beat. *J Physiol* 1887;8:229–234.

2. Einthoven W. The different forms of the human electrocardiogram and their signification. *Lancet* 1912;1:853–861 [reprinted in *Am Heart J* 1950;40:195–211].

3. Einthoven W, Fahr G, de Waart A. Über die Richtung und die manifeste Grösse der Potentialschwankungen im menschlichen Herzen und über den Einfluss der Herzlage auf die Form des Elektrokardiogramms. *Pflügers Arch* 1913;150:175–315 (Translation: Hoff HE, Sekelj P. *Am Heart J* 1957;40:163–194).

4. Wilson FN, Johnston FD, MacLeod AG, Barker PS. Electrocardiograms that represent the potential variations of a single electrode. *Am Heart J* 1934;9:447-458.

5. Bacharova L, Selvester RH, Engblom H, Wagner GS. Where is the central terminal located? In search of understanding the use of the *Wilson central terminal* for production of 9 of the standard 12 electrocardiogram leads. *J Electrocardiol* 2005;38:119-127.

6. Barnes AR, Pardee HEB, White PD, Wilson FN, Wolferth CC, Bedford DE; Cowan J, Drury AN, Hill IGW, et al. Standardization of precordial leads: Joint recommendations of the American Heart Association and the Cardiac Society of Great Britain and Ireland. *Am Heart J* 1938;15:107–108.

7. Barnes AR, Pardee HEB, White PD, Wilson FN, Wolferth CCl. Standardization of precordial leads: Supplementary report. Committee of the American Heart Association for the Standardization of Precordial Leads. *Am Heart J* 1938;15:235–239.

8.  Goldberger E. A simple, indifferent, electrocardiographic electrode of zero potential and a technique of obtaining augmented, unipolar, extremity leads. *Am Heart J* 1942;23:483–492.

9.  Anderson ST, Pahlm O, Selvester RH, Bailey JJ, Berson AS, Barold SS, Clemmensen P, Dower GE, Elko PP, et al. Panoramic display of the orderly sequenced 12-lead ECG. *J Electrocardiol* 1994;27:347–352.

10. Frank E. An accurate, clinically practical system for spatial vectorcardiography. *Circulation* 1956;13:737–749.

11. Frank E. The image surface of a homogeneous torso. *Am Heart J* 1954;47:757–768.

12. Dower GE, Bastos Machado H, Osborne JA. On deriving the electrocardiogram from vectorcardiographic leads. *Clin Cardiol* 1980;3:87–95.

13. Dower GE, Yakush A, Nazzal SB, Jutzy RV, Ruiz CE. Deriving the 12-lead electrocardiogram from four (EASI) electrodes. *J Electrocardiol* 1998;21(Suppl):182–187.

14. Feild DQ, Feldman CL, Horáček BM. Improved EASI coefficients: Their derivation, values, and performance. *J Electrocardiol* 2002;35(Suppl):23–33.

15. Edenbrandt L, Pahlm O, Sörnmo L. An accurate exercise lead system for bicycle ergometer tests. *Eur Heart J* 1989;10:268–272.

16. Pahlm O, Haisty WK, Edenbrandt L, Wagner NB, Sevilla DC, Selvester RH, Wagner GS. Evaluation of changes in standard electrocardiographic QRS waveforms recorded from activity-compatible proximal limb lead positions. *Am J Cardiol* 1992;69:253–257.

17. Papouchado M, Walker PR, James MA, Clarke LM. Fundamental differences between the standard 12-lead electrocardiogram and the modified (Mason-Likar) exercise lead system. *Eur Heart J* 1987;8:725–733.

18. Drew BJ, Scheinmn MM, Evans GT. Comparison of a vectorcardiographically derived 12-lead electrocardiogram with the conventional electrocardiogram during wide QRS complex tachycardia, and its potential application for continuous bedside monitoring. *Am J Cardiol* 1992;69:612–618.

19. Drew BJ, Pelter MM, Wung S-F, Adams MG, Taylor C, Evans GT, Foster E. Accuracy of the EASI 12-lead electrocardiogram compared to the standard 12–lead electrocardiogram for diagnosing multiple cardiac abnormalities. *J Electrocardiol* 1999;32(Suppl):38–47.

20. Drew BJ, Adams MG, Pelter MM, Wung S-F, Caldwell MA. Comparison of standard and derived 12-lead electrocardiograms for diagnosis of coronary angioplasty-induced myocardial ischemia. *Am J Cardiol* 1997;78:639–644.

21. Feldman CL, MacCallum G, Hartley LH. Comparison of the standard ECG with the EASI cardiogram for ischemia detection during exercise monitoring. *Comput Cardiol* 1997;24:343–345.

22. Klein MD, Key-Brothers I, Feldman CL. Can the vectorcardiographically derived EASI ECG be a suitable surrogate for the standard ECG in selected circumstances? *Comput Cardiol* 1997;24:721–724.

23. Horáček BM, Warren JW, Štóvíček P, Feldman CL. Diagnostic accuracy of derived versus standard 12-lead electrocardiograms. *J Electrocardiol* 2000;33(Suppl):155–160.

24. Denes P. The importance of derived 12-lead electrocardiography in the interpretation of arrhythmias detected by Holter monitoring. *Am Heart J* 1992;124:905–911.

25. Mason RE, Likar I. A new system of multiple-lead exercise electrocardiography. *Am Heart J* 1966;71:196–205.

26. Wilson FN. The distribution of the potential differences produced by the heart beat within the body and at its surface. *Am Heart J* 1930;5:599–616.

27. Waller AD. On the electromotive changes connected with the beat of the mammalian heart and of the human heart in particular. *Philos Trans R Soc London B Biol Sci* 1889;180:169–194.

28. Kornreich F, Rautaharju PM, Warren J, Montague TJ, Horáček BM. Identification of best electrocardiographic leads for diagnosing myocardial infarction by statistical analysis of body surface potential maps. *Am J Cardiol* 1985;56:852–856.

29. Kornreich F, Montague TJ, Rautaharju PM, Kavadias M, Horáček BM. Identification of best electrocardiographic leads for diagnosing left ventricular hypertrophy by statistical analysis of body surface potential maps. *Am J Cardiol* 1988;62:1285–1291.

30. Yamada K, Toyama J, Wada M, Sugiyama S, Sugenoya J. Body surface isopotential mapping in Wolff-Parkinson-White syndrome: Noninvasive method to determine the localization of the accessory atrioventricular pathway. *Am J Cardiol* 1975;90:721–734.

31. Carley SD, Jenkins M, Jones KM. Body surface mapping versus the standard 12-lead ECG in the detection of myocardial infarction amongst emergency department patients: A Bayesian approach. *Resuscitation* 2004;64:309–314.

32. Selvester RH, Wagner GS, Hindman NB. The Selvester QRS scoring system for estimating myocardial infarct size. The development and application of the system. *Arch Intern Med* 1985;145:1877–1881.

33. Selvester RH, Wagner JO, Rubin HB. Quantitation of myocardial infarct size and location by electrocardiogram and vectorcardiogram. In: Snellin HA, ed. *Boerhave Course in Quantitation in Cardiology*. Leyden, The Netherlands: Leyden University Press; 1972:31–44.

34. Wagner GS, Freye CJ, Palmeri ST, Roark SF, Stack NC, Ideker RE, Harrell FE, Selvester RH. Evaluation of a QRS scoring system for estimating myocardial infarct size. I. Specificity and observer agreement. *Circulation* 1982;65:342–347.

35. Ideker RE, Wagner GS, Ruth WK, Alonso DR, Bishop SP, Bloor CM, Fallon JT, Gottlieb GJ, et al. Evaluation of a QRS scoring system for estimating myocardial infarct size. II. Correlation with quantitative anatomic findings for anterior infarcts. *Am J Cardiol* 1982;49:1604–1614.

36. Roark SF, Ideker RE, Wagner GS, Alonso DR, Bishop SP, Bloor CM, Bramlet DA, Edwards JE, Fallon JT, et al. Evaluation of a QRS scoring system for estimating myocardial infarct size. III. Correlation with quantitative anatomic findings for inferior infarcts. *Am J Cardiol* 1983;51:382–389.

37. Ward RM, White RD, Ideker RE, Hindman NB, Alonso DR, Bishop SP, Bloor CM, Fallon JT, Gottlieb GJ, et al. Evaluation of a QRS scoring system for estimating myocardial infarct size. IV. Correlation with quantitative anatomic findings for posterolateral infarcts. *Am J Cardiol* 1984;53:706–714.

38. Hindman NB, Schocken DD, Widmann M, Anderson WD, White RD, Leggett S, Ideker RE, Hinohara T, Selvester RH, Wagner GS. Evaluation of a QRS scoring system for estimating myocardial infarct size. V. Specificity and method of application of the complete system. *Am J Cardiol* 1985;55:1485–1490.

39. Sevilla DC, Wagner NB, White RD, Peck SL, Ideker RE, Hackel DB, Reimer KA, Selvester RH, Wagner GS. Anatomic validation of electrocardiographic estimation of the size of acute or healed myocardial infarcts. *Am J Cardiol* 1990;65:1301–1307.

40. Sevilla DC, Wagner NB, Pegues R, Peck S, Mikat E, Ideker R, Hutchins G, Reimer K, Hackel D, Selvester R, Wagner GS. Correlation of the complete version of the Selvester QRS scoring system with quantitative anatomic findings for multiple left ventricular myocardial infarcts. *Am J Cardiol* 1992;69:465–469.

41. Engblom H, Wagner GS, Setser RM, Selvester RH, Billgren T, Kasper JM, Maynard C, Pahlm O, Arheden H, White RD. Quantitative clinical assessment of chronic anterior myocardial infarction with delayed enhancement magnetic resonance imaging and QRS scoring. *Am Heart J* 2003;146:359–366.

42. Horáček BM, Warren JW, Albano A, Palmeri MA, Rembert JC, Greenfield JC Jr, Wagner GS. Development of an automated Selvester Scoring System for estimating the size of myocardial infarction from the electrocardiogram. *J Electrocardiol* 2006;39:162–168.

43. Wagner GS, Greenfield JC Jr, Rembert JC, Warren JW, Albano A, Palmeri MA, Horáček BM. Comparison of the Selvester QRS scoring system applied on standard versus high-resolution electrocardiographic recordings. *J Electrocardiol* 2007;40:288–291.

44. Strauss DG, Selvester RH. The QRS complex – a biomarker that "images" the heart: QRS scores to quantify myocardial scar in the presence of normal and abnormal ventricular conduction. *J Electrocardiol* 2009;42:85–96.

45. Macfarlane P. Normal limits. In: P Macfarlane, T Lawrie, eds. *Comprehensive Electrocardiology: Theory and Practice in Health and Disease*. Vol. 3. 1st ed. New York: Pergamon Press; 1989:1441–1526.

46. Pahlm O, Haisty WK Jr, Wagner NB, Pope JE, Wagner GS. Specificity and sensitivity of QRS criteria for diagnosis of single and multiple myocardial infarcts. *Am J Cardiol* 1991;68:1300–1304.

47. Selvester RH, Wagner GS, Ideker RE, Gates K, Starr S, Ahmed J, Crump R. ECG myocardial infarct size: a gender-, age, race-insensitive 12-segment multiple regression model. I: Retrospective learning set of 100 pathoanatomic infarcts and 229 normal control subjects. *J Electrocardiol* 1994; 27(Suppl):31–41.

48. Kim RJ, Fieno DS, Parrish TB, Harris K, Chen EL, Simonetti O, Bundy J, Finn JP, Klocke FJ, Judd RM. Relationship of MRI delayed contrast enhancement to irreversible injury, infarct age and contractile function. *Circulation* 1999;100:1992–2002.

49. Tong CY, Prato FS, Wisenberg G, Lee TY, Carroll E, Sandler D, Wills J, Drost D. Measurement of the extraction efficiency and distribution volume for Gd-DTPA in normal and diseased canine myocardium. *Magn Reson Med* 1993;30:337–346.

50. Saeed M, Wendland MF, Masui T, Higgins CB. Reperfused myocardial infarctions on T1- and susceptibility-enhanced MRI: evidence for loss of compartmentalization of contrast media. *Magn Reson Med* 1994;31:31–39.

51. Arheden H, Saeed M, Higgins CB, Gao DW, Bremerich J, Wyttenbach R, Dae MW, Wendland MF. Measurement of the distribution volume of gadopentetate dimeglumine at echo-planar MR imaging to quantify myocardial infarction: comparison with 99mTc-DTPA autoradiography in rats. *Radiology* 1999;211:698–708.

52. Flacke SJ, Fischer SE, Lorenz CH. Measurement of the gadopentetate dimeglumine partition coefficient in human myocardium in vivo: normal distribution and elevation in acute and chronic infarction. *Radiology* 2001;218:703–710.

53. Simonetti OP, Kim RJ, Fieno DS, Hillenbrand HB, Wu E, Bundy JM, Finn JP, Judd RM. An improved MR imaging technique for the visualization of myocardial infarction. *Radiology* 2001;218:215–223.

54. Kim RJ, Wu E, Rafael A, Chen EL, Parker MA, Simonetti O, Klocke FJ, Bonow RO, Judd RM. The use of contrast-enhanced magnetic resonance imaging to identify reversible myocardial dysfunction. *N Engl J Med* 2000;343:1445–1453.

55. Heiberg E, Ugander M, Engblom H, Gotberg M, Olivecrona GK, Erlinge D, Arheden H. Automated quantification of myocardial infarction from MR images by accounting for partial volume effects: animal, phantom, and human study. *Radiology* 2008;246:581–588.

56. Engblom H, Hedström E, Heiberg E, Wagner GS, Pahlm O, Arheden H. Rapid initial reduction of hyperenhanced myocardium after reperfused first myocardial infarction suggests recovery of the peri-infarction zone: one-year follow-up by MRI. *Circ Cardiovasc Imaging* 2009;2:47–55.

57. Oshinski JN, Yang Z, Jones JR, Mata JF, French BA. Imaging time after Gd-DTPA injection is critical in using delayed enhancement to determine infarct size accurately with magnetic resonance imaging. *Circulation* 2001;104:2838–2842.

58. Engblom H, Arheden H, Foster JE, Martin TN. Myocardial infarct quantification: Is magnetic resonance imaging ready to serve as gold standard for electrocardiology? *J Electrocardiol* 2007;40:243–245.

59. Lopez AD, Mathers CD, Ezzati M, Jamison DT, Murray CJL. Global and regional burden of disease and risk factors, 2001: systematic analysis of population health data. *Lancet* 2006;367:1747–1757.

60. Stene MCA, Frikke-Schmidt R, Nordestgaard BG, Grande P, Schnohr P, Tybjærg-Hansen A. Functional promotor variant in zinc finger protein 202 predicts severe atherosclerosis and ischemic heart disease. *J Am Coll Cardiol* 2008;52:369–377.

61. Ross R. Atherosclerosis – an inflammatory disease. *N Engl J Med* 1999;340:115–126.

62. Glass CK, Witztum JL. Atherosclerosis: The road ahead. *Cell* 2001;104:503–516.

63. Braunwald E, Antman EM, Beasley JW, Califf RM, Cheitlin MD, Hochman JS, Jones RH, Kereiakes D, Kupersmith J, et al. ACC/AHA guidelines for the management of patients with unstable angina and non–ST-segment elevation myocardial infarction: Executive summary and recommendations: A report of the American College of Cardiology/American Heart Association Task Force on Practice Guidelines (Committee on the Management of Patients With Unstable Angina). *Circulation* 2000;102:1193–1209.

64. Martin TN, Groenning BA, Murray HM, Steedman T, Foster JE, Elliot AT, Dargie HJ, Selvester RH, Pahlm O, Wagner GS. ST-segment deviation analysis of the admission 12-lead electrocardiogram as an aid to early diagnosis of acute myocardial infarction with a cardiac magnetic resonance imaging gold standard. *J Am Coll Cardiol* 2007;50:1021–1028.

65. Macfarlane PW. Evolution of the Glasgow program for computer-assisted reporting of electrocardiograms—1964/1998. *Acta Cardiol* 1998;53:117–120.

66. Macfarlane PW, Devine B, Clark E. The university of Glasgow (Uni-G) ECG analysis program. *Comput Cardiol* 2005;32:451–454.

67. Tarvainen MP, Ranta-Aho PO, Karjalainen PA. An advanced detrending method with application to HRV analysis. *IEEE Trans Biomed Eng* 2002;49:172–175.

68. Horáček BM, Warren JW, Penney CJ, MacLeod RS, Title LM, Gardner MJ, Feldman CL. Optimal electrocardiographic leads for detecting acute myocardial ischemia. *J Electrocardiol* 2001;34(Suppl):97–111.

69. Anderson WD, Wagner NB, Lee KL, White RD, Yuschak J, Behar VS, Selvester RH, Ideker RE, Wagner GS. Evaluation of a QRS scoring system for estimating myocardial infarct size. VI: Identification of screening criteria for non-acute myocardial infarcts. *Am J Cardiol* 1988;61:729–733.

70. Altman DG. *Practical Statistics for Medical Research*. London: Chapman and Hall; 1991:403–407.

71. Bland JM, Altman DG. Statistical methods for assessing agreement between two methods of clinical measurement. *Lancet* 1986;1:307–310.

72. Holmvang L, Hasbak P, Clemensen P, et al. Differences between local investigator and core laboratory interpretation of the admission electrocardiogram in patients with unstable angina pectoris or non-Q-wave myocardial infarction (a ThRombin Inhibition in Myocardial Ischemia [TRIM] substudy). *Am J Cardiol* 1998;82:54–60.

73. Sokolove PE, Sgarbossa EB, Amsterdam EA, Gelber R, Lee TC, Maynard C, Richards JR, Valente R, Wagner GS. Interobserver agreement in the electrocardiographic diagnosis of acute myocardial infarction in patients with left bundle branch block. *Ann Emerg Med* 2000;36:566–571.

# Acknowledgments

I am most grateful for all the help and encouragement that I have received on my way towards my PhD. I would like to thank all those who have supported me during this time, without whom this thesis would never have been possible. I would especially like to thank:

**Olle Pahlm**, my supervisor, for all your support, and for making me persist during difficult times. It has been a privilege to share your enormous knowledge and experience.

**Galen Wagner**, my cosupervisor, for your advice and help, for many memorable and rewarding discussions, and for your great hospitality in Durham.

**Håkan Arheden**, for providing many interesting aspects of leadership and life in general.

**Björn Jonson**, for providing insight into the academic world.

**Charles Maynard**, for all your help with statistical analysis.

**Leif Sörnmo**, for your help in the field of signal processing.

**Henrik Engblom**, for all your help with MRI and statistics, and for your contributions to Study V.

**Erik Hedström**, for your help with MRI.

**Kerstin Brauer**, for your excellent help with illustrations and manuscripts.

**Britt-Marie Gunnarsson**, for all your technical help.

**Linda Lim**, **Arzu Glave**, **Ronny Qvist**, and **Madeleine Robinson** for your help with ECG recording and enrollment of patients.

**Lisbeth Nilsson** and **Gunnel Hansson**, for your help with ECG recording.

**Madeleine Nilsson,** for your contribution to Study V.

**Bo Hedén,** for your contribution to Study V.

All my **coauthors**, for your contributions.

**Elin Trägårdh-**Johansson, for your support and great friendship, especially during travels.

**Karin Larsson**, **Märta Granbohm**, **Kathy Shuping**, and **Beverly Perkins**, for secretarial assistance.

Staff and colleagues at the **Department of Clinical Physiology**, for your understanding and support, and for making it possible for me to use my research time.

My dear parents, **Karin** and **Thomas**, for your love and support, for always caring and believing in me, and for all your help with Zackarias and Adam when both Linus and I have been working late.

Finally, my beloved husband **Linus**, and my 2 miracles, my wonderful sons **Zackarias** and **Adam**, for all your love, support, and patience and for letting me share my life with you.

# Papers I–V